Comparative Biochemistry and Physiology, Part B 193 (2016) 33–46

Contents lists available at ScienceDirect

Comparative Biochemistry and Physiology, Part B

journal homepage: www.elsevier.com/locate/cbpb

Adjustments of molecular key components of branchial ion and pH regulation in Atlantic cod (*Gadus morhua*) in response to ocean acidification and warming

Katharina Michael [a], Cornelia M. Kreiss [a], Marian Y. Hu [b,1], Nils Koschnick [a], Ulf Bickmeyer [a], Sam Dupont [b], Hans-O. Pörtner [a], Magnus Lucassen [a,*]

[a] Alfred Wegener Institute, Helmholtz Center for Polar and Marine Research, 27570 Bremerhaven, Germany
[b] Department of Biological and Environmental Sciences, University of Gothenburg, The Sven Lovén Centre for Marine Sciences, Kristineberg, 45178 Fiskebäckskil, Sweden

ARTICLE INFO

Article history:
Received 8 September 2015
Received in revised form 8 December 2015
Accepted 8 December 2015
Available online 11 December 2015

Keywords:
Na^+/HCO_3^- co-transporter 1
NBC1
Fish gills
Marine teleost
Acid–base regulation

ABSTRACT

Marine teleost fish sustain compensation of extracellular pH after exposure to hypercapnia by means of efficient ion and acid–base regulation. Elevated rates of ion and acid–base regulation under hypercapnia may be stimulated further by elevated temperature. Here, we characterized the regulation of transepithelial ion transporters (NKCC1, NBC1, SLC26A6, NHE1 and 2) and ATPases (Na^+/K^+ ATPase and V-type H^+ ATPase) in gills of Atlantic cod (*Gadus morhua*) after 4 weeks of exposure to ambient and future PCO_2 levels (550 μatm, 1200 μatm, 2200 μatm) at optimum (10 °C) and summer maximum temperature (18 °C), respectively. Gene expression of most branchial ion transporters revealed temperature- and dose-dependent responses to elevated PCO_2. Transcriptional regulation resulted in stable protein expression at 10 °C, whereas expression of most transport proteins increased at medium PCO_2 and 18 °C. mRNA and protein expression of distinct ion transport proteins were closely co-regulated, substantiating cellular functional relationships. Na^+/K^+ ATPase capacities were PCO_2 independent, but increased with acclimation temperature, whereas H^+ ATPase capacities were thermally compensated but decreased at medium PCO_2 and 10 °C. When functional capacities of branchial ATPases were compared with mitochondrial F_1F_o ATP-synthase strong correlations of F_1F_o ATP-synthase and ATPase capacities generally indicate close coordination of branchial aerobic ATP demand and supply. Our data indicate physiological plasticity in the gills of cod to adjust to a warming, acidifying ocean within limits. In light of the interacting and non-linear, dose-dependent effects of both climate factors the role of these mechanisms in shaping resilience under climate change remains to be explored.

1. Introduction

The anthropogenic changes of temperature and atmospheric CO_2 concentrations in global climate are inevitably linked. Depending on the emission scenario employed, atmospheric CO_2 is projected to reach 421 μatm to 936 μatm by the year 2100 and about 2000 μatm after 2250 under business as usual emissions (Meinshausen et al., 2011; IPCC, 2013). By the year 2100 and compared to the 1950s this increase in PCO_2 is projected to be accompanied by an average decrease in oceanic surface water pH by 0.14–0.32 pH units and by another 0.8 to 1.4 pH units by the year 2300 (Caldeira and Wickett, 2005; IPCC, 2013). Furthermore, models agree on continued global ocean warming, although patterns differ in the magnitudes of both global as well as regional changes (Collins et al., 2013).

Elevated ambient PCO_2 (hypercapnia) alters the PCO_2 gradient from aquatic animals to their environment and thus, affects CO_2 release (Heuer and Grosell, 2014). The sensitivity of fish to hypercapnia was proposed to be lower than that of most invertebrates due to the higher capacity of fish to regulate acid–base homeostasis (Melzner et al., 2009b). When exposed to hypercapnia, marine teleost fish accomplish full and sustained compensation of the initial respiratory acidosis within the first 24–72 h, a process that includes the production, uptake and excretion of acid–base relevant ions, primarily at the gills (Claiborne et al., 2002; Brauner et al., 2004; Evans et al., 2005). However, acid–base status and ion equilibria reach new steady state values which may lead to other downstream consequences or trade-offs (see Heuer and Grosell, 2014 for review).

Generally, teleost ion and acid–base regulation is mainly achieved in specialized gill cells (ionocytes) and involves multiple transport proteins and signaling pathways. Additionally, the roles of the transporters

* Corresponding author at: Alfred Wegener Institute, Helmholtz Center for Polar and Marine Research (AWI), Am Handelshafen 12, 27570 Bremerhaven, Germany.
E-mail address: Magnus.Lucassen@awi.de (M. Lucassen).
[1] Institute of Physiology, Christian-Albrechts-University Kiel, 24098 Kiel, Germany.

http://dx.doi.org/10.1016/j.cbpb.2015.12.006

involved in both osmotic as well as acid–base regulation are intertwined (Pritchard, 2003; Marshall and Grosell, 2006). Marine fish constantly counteract the osmotic water loss to their hyperosmotic environment by drinking, i.e. absorbing salt and water across the gastrointestinal tract and actively secreting the surplus salt load at the gills. Cl^- enters the branchial cell via the $Na^+/K^+/Cl^-$ co-transporter 1 (NKCC1) driven by the Na^+ gradient, which is provided by the Na^+/K^+ ATPase, and is secreted at the apical membrane through CFTR type (cystic fibrosis transmembrane conductance regulator) anion channels. Na^+ follows passively through paracellular tight junction pathways (see e.g. Evans et al., 2005; Hiroi and McCormick, 2012; Hwang et al., 2011; Marshall and Grosell, 2006). Plasma pH is adjusted by the net accumulation of HCO_3^- in the body fluids and a net secretion of acid equivalents into the environment, as respiratory adjustments are relatively ineffective to compensate for pH disturbances in water breathers (Claiborne et al. (2002), reviewed by Perry and Gilmour (2006)). According to the current models proposed for branchial marine fish acid–base transport (see e.g. Esbaugh et al., 2012; Heuer and Grosell, 2014; Hwang et al., 2011), protons are excreted into the surrounding seawater across the gill epithelium predominantly via apical Na^+/H^+ exchangers (NHE; SLC9; isoform 2 and 3). Furthermore, basolateral NHE (isoform 1) as well as H^+ ATPase were proposed to contribute to acid–base regulation in marine fish. Bicarbonate transport is achieved in exchange for chloride via anion exchangers (AE; SLC4, isoform 1 and 2) on both sides of the epithelium as well as via a Na^+/HCO_3^- co-transporter 1 (NBC1, SLC4, isoform 4) on the basolateral side. Additionally, members of the Cl^-/HCO_3^- exchanger (SLC26) protein family may be involved in branchial bicarbonate transport.

In the past, studies of acid–base regulation in marine fish under environmental hypercapnia have focused on the identification of relevant mechanisms. However, relatively high PCO_2 levels have been applied (Larsen et al., 1997; Michaelidis et al., 2007; Perry et al., 2010). During a time series of 6 weeks under hypercapnia (≥10,000 μatm), shifting acclimation patterns in mRNA and protein expression of branchial ion transporters were found in the common eelpout (Deigweiher et al., 2008). Furthermore, Na^+/K^+ ATPase densities and capacities increased long-term, indicating elevated rates of ion and acid–base regulation under hypercapnia in gills of common eelpout (Deigweiher et al., 2008) and Atlantic cod, respectively (Melzner et al., 2009a). The need to compensate for the effects of elevated PCO_2 on passive and active branchial ion transport processes might be enhanced by elevated temperature and involve augmented metabolic costs of ion regulation. As defending extracellular pH may be a key factor in shaping the physiological resilience of marine ectotherms to global climate change (Pörtner, 2008), it is critical to understand the contribution of ion and acid–base regulation to resilience in response to both, projected PCO_2 and temperature levels (Pörtner, 2008, 2012).

The present work aims to analyze the responses of key ion and acid–base regulatory mechanisms to elevated PCO_2 and temperature in gills of Atlantic cod (*G. morhua*), a marine fish of high ecological and commercial importance. The species has a pan-Atlantic distribution and, depending on the season and the respective population, experiences habitat temperatures ranging from −1 °C to 19 °C (Righton et al., 2010). In our experiments, Atlantic cod from the Skagerrak/Kattegat (Gullmarsfjord, Sweden) population were exposed to PCO_2 levels covering present and future natural variability at the study site (550 μatm (low), 1200 μatm (medium) and 2200 μatm (high); Dorey et al. (2013)) at 10 °C and 18 °C for four weeks, respectively. 10 °C constitutes the average habitat temperature and is close to the thermal optimum of growth, whereas 18 °C is close to the summer maximum experienced by this population (Pörtner et al., 2001; Righton et al., 2010). Cellular localization of Na^+/K^+ ATPase and its co-localization with NKCC1 and NBC1 was assessed in order to obtain insight into the functional relationship of these ion transport proteins in marine fish ionocytes. The expression of ion transporters such as $Na^+/K^+/Cl^-$ co-transporter 1 (NKCC1), Na^+/HCO_3^- co-transporter 1 (NBC1), Na^+/H^+ exchanger 1 and 2 (NHE1 and NHE2) as well as of one member of the anion transporter family SLC26 (member A6, SLC26A6) was characterized at transcriptional and translational level. The capacities of ATP-dependent ion pumps (Na^+/K^+ ATPase and V-type H^+ ATPase; H^+ ATPase in the following) were determined at mRNA, protein and functional level as well as in relation to the ATP-producing mitochondrial F_1F_o ATP-synthase in order to detect possible impacts on the branchial energy budget.

2. Material and methods

2.1. Ethical procedures

All experiments were conducted in compliance with the Swedish animal welfare legislation and approved by the Swedish ethical committee on animal experiments (reference number: Dnr 23-2012).

2.2. Animals

Atlantic cod of mixed gender (200.52 ± 95.4 g FW) (*G. morhua*) were caught in traps during February and March 2012 and kept at the Sven Lovén Centre for Marine Sciences, Kristineberg, Sweden in flow-through tank systems supplying seawater directly from the Gullmarsfjord at 10 °C. For the exposure experiment, 8–10 fish per treatment were slightly anesthetized with MS-222 (<0.2 g l^{-1}) and tagged individually (Visible Implant Elastomer, Northwest Marine Technology Inc., USA) after recording individual length and weight. After one week of recovery, fish were incubated in 2 replicate aquaria systems for four weeks at 10 °C and 18 °C and nominal PCO_2 levels of 550 μatm (low), 1200 μatm (medium) and 2200 μatm (high), respectively. Fish reared at low PCO_2 were maintained in aerated natural seawater. Water PCO_2 and associated pH values of each aquarium system were maintained by a pH titration system controlling the inflow of CO_2 gas (Aqua Medic, Bissendorf, Germany). Water temperature was kept constant by a computer controlled heating system integrated into the station's pump system. Additionally, online recordings (ProfiLux, GHL, Kaiserslautern, Germany) of salinity, temperature and pH confirmed stable conditions in all 12 tanks. Water chemistry was controlled twice a week by measuring pH (WTW portable pH meter ProfiLine pH 3310, NBS scale corrected to total scale via Dickson standards), alkalinity, total dissolved inorganic carbon (DIC) (Seal Analysis SFA QuAAtro; 800 TM), salinity (WTW conductivity meter Cond1970i) and temperature. PCO_2 values were calculated using the CO_2sys program (Pierrot, D. E. Lewis, and D. W. R. Wallace, 2006, MS Excel Program Developed for CO_2 System Calculations). See Kreiss et al. (2015b) for seawater chemistry and temperatures in all 12 tanks as well as for statistical analysis of experimental conditions. Fish were maintained under a 12:12 day:night cycle and fed three times a week until satiation with frozen shrimp and blue mussel. Animals were starved for 48 h prior to sampling. Individual fish were anesthetized with MS-222 (0.2 g l^{-1}), and length and weight were determined. Blood samples were drawn from the ventral vein, and fish were killed by a cut through their spine as close to the cranium as possible. Gill arches were dissected first, the gill tissue was separated from the arches, shock-frozen in liquid nitrogen and stored at −80 °C. 10 fish per treatment (5 per replicate tank) were randomly chosen for the analysis. Consecutively, gill tissue samples used in this study originate from individual fish (n = 10, 5 per replicate tank). For each analysis (mRNA expression, protein expression and enzyme activities), tissue aliquots were taken from the same individual. For the detection of potential differences between replicates, unpaired t-tests were performed. Unfortunately, fish from the two replicate tanks at 18 °C and low PCO_2 could not be clearly assigned to their original tank as these were accidentally mixed. For the remaining groups, no differences in any of the tested parameters were detected between replicate tanks. Total mortality during the experiment was 8.2% (9 fish) (see also Kreiss et al., 2015b).

2.3. mRNA expression of ion transporters

Total RNA from gill tissue (see Animals section for respective sampling design) was isolated using RNeasy Mini Kit (Qiagen, Hilden, Germany). Deep-frozen tissue samples were homogenized using the Precellys tissue homogenizer at 5000 rpm (3 × 15 s interrupted by a 10 s pause in between) (Peqlab, Erlangen, Germany). Tissue extracts were further processed according to the manufacturer's instructions. The complete removal of DNA was ensured by DNase digestion (Turbo DNA-free Kit; Life Technologies, Darmstadt, Germany). DNA-free total RNA was transcribed into cDNA (0.1 μg DNA-free total RNA) with the High-Capacity cDNA-RT Kit (Life Technologies, Darmstadt, Germany) to serve as a DNA template for large scale quantitative real-time PCR (qPCR) (TaqMan® OpenArray® Real-time PCR). Concentration and urity of the total RNA and DNA-free total RNA were controlled using NanoDrop (NanoDrop 2000, Peqlab, Erlangen, Germany). Mean total gill tissue RNA content [μg mg fwt^{-1}] is given in Table 1.

2.4. Array design

A set of essential ion regulatory transporters was compiled based on literature data. Sequences of those transporters were obtained by searching the published cod genome (Star et al., 2011) by annotations. Sequences not available in the cod genome were obtained by using sequences known from other fish species as query sequences against the EST database of NCBI (www.ncbi.nlm.nih.gov/dbEST/; restricted to tax ID = 8048; *G. morhua*). The respective blast hits were verified and further processed employing the MacVector software (version 10.0.2, MacVector Inc.). Isoforms were identified using the phylogenetic analysis tool of the MacVector software including known isoform sequences from various phyla. Reference genes were chosen according to Olsvik et al. (2008). Additionally, 18S-rRNA (Lucassen et al., 2006) was included as reference gene. Furthermore, all sequence annotations were double-checked by reverse blast (rpstblastn) against the fiNOG-database (Windisch et al., 2012) and against the nucleotide collection (nr) database using the blast2GO software (b2GO: Conesa et al., 2005; fiNOG: eggnog Version 3, Powell et al., 2012). The longest sections without unknowns were validated again (blast2GO) and used for primer and probe design. Sequences used were further re-validated against the cod genome annotation (Flicek et al., 2014; ENSEMBL, Wellcome Trust Sanger Institute/European Bioinformatics Institute). Primer/probe design and chip loading (array format 112) was performed by Life Technologies (Darmstadt, Germany). A final list of the genes analyzed and the corresponding primer and probe sequences is given in Table 2.

2.5. TaqMan® OpenArray® Real-time PCR

Large scale TaqMan® based quantitative real-time PCR was performed on an OpenArray® system (Life Technologies, Darmstadt, Germany) according to the manufacturer's protocol. qPCR reactions were premixed in a 96 well plate containing 100 ng/μl cDNA and 12.5 μl Master Mix (TaqMan® OpenArray® Gene Expression Master Mix). After mixing, 5 μl were transferred to the OpenArray® 384-well sample plates. Chip loading (33 nl each) was conducted by the OpenArray® AccuFill™ system. All samples were run in duplicate. No-template controls (NTC) and no-reverse-transcription (-RT) RNA controls were also implemented. Pooled control samples (10 °C, low PCO_2) were used as internal calibration for every chip.

Table 1
Mean total DNA-free RNA [μg mg fresh weight^{-1}] and protein [mg g fresh weight^{-1}] content in gill tissue of Atlantic cod (*G. morhua*) acclimated to 550 μatm, 1200 μatm and 2200 μatm CO_2 and 10 °C or 18 °C, respectively. Post-hoc tests only tested for significant differences within acclimation temperatures and PCO_2 levels. Different letters denote significant differences between PCO_2 treatments at 10 °C (a/b) and 18 °C (A/B), whereas a hash key indicates differences between acclimation temperatures at 550 μatm, 1200 μatm and 2200 μatm, respectively. n = 7–10 per treatment. Values are depicted as means ± SEM.

		Protein content	DNA-free RNA content
		[mg g fwt^{-1}]	[μg mg fwt^{-1}]
10 °C	550 μatm	45.30 ± 2.13	1.62 ± 0.12$^{A\#}$
	1200 μatm	47.28 ± 5.45	1.30 ± 0.12$^{AB\#}$
	2200 μatm	43.49 ± 2.52	1.22 ± 0.06^{B}
18 °C	550 μatm	40.45 ± 5.15	0.84 ± 0.09
	1200 μatm	43.76 ± 2.61	0.69 ± 0.09
	2200 μatm	37.00 ± 2.68	0.97 ± 0.11

2.6. OpenArray® data processing

OpenArray® system output files were reassembled and genes expressing none or out of range signals in all samples were excluded from further analysis. Each array (one gene and one sample in duplicates) was checked manually to exclude technical errors. Data points not available because of technical failures were replaced with the tissue and treatment specific mean Ct value. From the 112 pre-chosen genes, 7 genes were designated as reference genes and the most stable reference genes under the experimental conditions were determined using the NormFinder package for R (Andersen et al., 2004), calculating the expression stability measure for each reference gene and determining the most stable combination of two genes (UBI and RPL22). Threshold cycle (Ct) values of the 10 genes analyzed in the course of this study were transformed into relative quantities for each gene *G* and sample *j*, ($\Delta Ct = E\hat{}$ (minimum $Ct_G - Ct_{Gj}$). A sample specific normalization factor (NF) was calculated by geometric averaging of ΔCt values obtained for the two references genes (see above). Relative quantities of each sample were normalized to the sample-specific NF by division, calculating normalized relative quantities (NRQs). NRQs were related to total gill tissue RNA content [μg mg fwt^{-1}; after DNAse treatment] and are given as NRQs per mg tissue fresh weight (NRQ mg fwt^{-1}). Data processing was performed using specifically developed R-scripts (R Core Team, 2014).

2.7. Protein quantification

Gill tissue samples (see Animals section for respective sampling design) were homogenized using a cooled tissue homogenizer (Precellys, Peqlab, Erlangen, Germany) at 5000 rpm (3 × 15 s interrupted by 10 s pause in between) in 10 volumes of ice-cold buffer per mg tissue weight as described by Deigweiher et al. (2008). One-half of the supernatant was used for Na^+/K^+ ATPase activity measurements and the other half for immunoblotting. For the validation of the specificity of primary antibodies, crude protein extracts of randomly chosen gill tissue samples were additionally separated by ultra-centrifugation (30 min at 350,000 *g* and 4 °C) into membrane and cytosolic fractions. Total protein contents were determined according to Bradford (1976), using BSA as standard. Total gill tissue protein content is given in Table 1. Slot blot immunoblotting was applied using a Hoefer PR 648 slot blot filtration system (Amersham Biosciences, Freiburg, Germany). Immuno-BlotTM PVDF membranes (Bio-Rad Laboratories) were pre-incubated in 100% methanol followed by equilibration in transfer buffer [10 mM $NaHCO_3$, 3 mM Na_2CO_3, 20% (v/v) methanol, 0.025% (w/v) sodium dodecyl sulfate (SDS), pH 9.5–9.9] for 30 min. To ensure an even distribution of the proteins in the slots, 5 μl crude extract were diluted 1:10 in electrophoresis running buffer [25 mM Tris, 192 mM glycine, 0.1% (w/v) SDS]. A dilution series of pooled control samples was used as an internal calibration standard on each membrane. Before application, protein extracts were randomized to avoid possible effects of the slot positions on the membranes. 50 μl of each sample were loaded by vacuum pressure, and slots were washed repeatedly with transfer buffer to ensure complete loading. The membrane was transferred instantaneously into TBS-Tween buffer [TBS-T; 50 mM Tris/HCl, pH 7.4, 0.9% (w/v) NaCl, 0.1% (v/v) Tween20] containing 5% (w/v) non-fat skimmed milk powder (blocking buffer) and blocked for 1 h at room temperature followed by incubation with the primary antibody (see Table 3) at 4 °C overnight. Blots were washed with TBS-T and

Table 2
Genes analyzed in the course of this study and the corresponding primer and probe sequences.

Gene ID	Annotation	Accession no.	Forward primer	Backward primer	TaqMan® Probe
18S^{+}	18S RNA	GMRRNA01	ATGGTGACCACGGGTAACG	CCTTGGATGTGGTAGCCATTTCTC	TCGAACCCTGATTCCC
ACTB^{+}	Beta-actin	EX739174	TGTCCCGAGGCCCTTTTC	TGGTCTCATGGATGCCACAAG	CAGCCCTCCTTCCTCG
RPLP1^{+}	Ribosomal protein lp1	EX741373	CTCATCAAGGCAGCTGGTGTAA	AGGGCCTTGGCGAAGAG	CCGTGGAGCCTTTCTG
RPL22^{+}	60s ribosomal protein l22	EX727868	ACCTGAAGTACCTCACCAAGAAGTA	CCACCACCCTCAGCCAATC	ACGCAGGTTGTTCTTC
RPL37^{+}	60s ribosomal protein l37	EX738140	CGAGAAGCGCAAGAGAAAGTATAAC	GCCAGTGGTGTTCCTCCTC	TTGGCCTTGGCACTCC
RPS9^{+}	40s ribosomal protein s9	EX726043	CTCACCCTGGACGAGAAAGAC	GACGTCTCAACAGAGCATTACCTT	CCCAAGCGTCTCTTTG
Ubi^{+}	Ubiquitin	EX735613	CCAGAAAGAGTCAACCCTGCAT	CATTCTGAGGGAAGGCTCAATGAT	CTGGTGCTCCGTCTGC
VHA-V1A	H^+ ATPase, V1 subunit A	ENSGMOG00000015627	GGGAACGAGATGTCGGAAGT	GTCCACCTCCATGGTAAGCT	CCTGCGAGACTTCCCA
ATNA1	Na^+/K^+ ATPase alpha 1	ES481707	ACGCAGAAAGATCGTAGAGTTTACTTG	CACTGGACCACCACGATACTG	CCACACGGCGTTCTT
ATNA2	Na^+/K^+ ATPase alpha 2a	ENSGMOG00000006554	ACGGAGCAGCTGTGCTT	CGGCGGAGCGACACTT	CTGGGCCTCATCTCC
ATNA3	Na^+/K^+ ATPase alpha 3b	ENSGMOG00000014788	TCCTTCCAGAACGCCTACATG	GCATCATAACCTGGCAGAAACC	AAGCACTCGCTCTCCC
NBC1	SLC family 4, member 4	KT997471	GCTCCTCTGGGTCCTAAAGTC	CCACCAGAGCCAGGATCATG	CCGCCATCGTATTCC
NHE1A	SLC family 9, member 1	ENSGMOG00000003996	TGGTCCCGCGGATGTG	TCTCGCTGTGCAGGTTGAAG	CCGTAGCCCGCCTCAG
NHE1B	SLC family 9, member 1	ENSGMOG00000012033	ACACGCGCGTCATCGA	CAGGTAGGCCATGTAGCTGTAC	CCGCTGTTCGTCTTCG
NHE2	SLC family 9, member 2	ENSGMOG00000012591	GCCGTCGGCACAGTGA	GGGACACCACGAAGAAGCA	ACGCCGTCCAGCACAG
NKCC1	SLC family 12, member 2	ENSGMOG00000004314	GCGTCATGTTCGTCATCAACT	GATGTACAGGCCCAAGACGAT	CAGCGCCGCCATCC
SLC26A6	SLC family 26, member 6	ENSGMOG00000009435	CTCAACGAGCGCTGCAA	GCCGTGGCGACGATGA	CCCCGGCGAGATCA

$^{+}$Reference gene.

incubated for 1 h with goat anti-mouse/anti-rabbit IgG antibody (Pierce, Rockford, IL, USA) diluted 1:20,000 in blocking buffer. Protein signals were visualized by using the ECL Advanced Western blotting detection reagent (GE Healthcare, Munich, Germany) and recorded by a cooled charge-coupled device camera (LAS-1000: Fuji, Tokyo, Japan). Signal intensity was calculated using the AIDA Image Analyzer software (version 3.52, Raytest, Straubenhardt, Germany). Results are expressed as arbitrary units per mg fresh weight (AU mg fwt^{-1}), recalculated from the calibration curves.

2.8. Development of cod (*G. morhua*) specific NBC1 antibody

A polyclonal antibody raised against NBC1 of Atlantic cod (*G. morhua*) was developed. A partial sequence for cod NBC1 was obtained by searching the *G. morhua* EST database at NCBI, and respective blast hits were verified and processed further employing the MacVector software (version 10.0.2, MacVector Inc.). The best hit (GO387248) was used as a template for the elongation of the 3′ end of the mRNA using RACE (rapid amplification of cDNA ends) technology (Life Technologies, Darmstadt, Germany) to obtain a potentially better antigenic peptide sequence within the hydrophilic C-terminal part of the protein. Position and sequences of the outer and inner 3′ RACE-primers are given in Table 4. 3′ RACE-PCR was conducted according to the manufacturer's protocol. RACE, cloning and analysis of PCR fragments were performed as described by Mark et al. (2006). Positive clones were sequenced commercially (Eurofins Genomics, Ebersberg, Germany) and the obtained contigs were assembled and processed further using MacVector revealing a 1564 bp DNA fragment, coding for the C-terminal part of NBC1. Compared to the ESTs used as a template (524 bp; see above), the obtained DNA fragment is elongated by 1041 bp and the respective open reading frame by 174 bp (stop codon at position 694 bp). The fragment contains a Poly-A signal sequence (5′-AAUAAA-3′) at position 1197 bp. The obtained sequence has been submitted to GenBank (accession number: KT997471). The peptide-specific cod NBC1 antibody was produced by Seqlab (Seqlab Sequence Laboratories, Göttingen, Germany) based on the peptide sequence derived from the cDNA sequence (aa 205 to 217; *EKEPFLGDKSFDK*).

2.9. Primary antibody specificity

For validation of the specificity of the primary antibodies used here, 10 μl of crude protein extract, cytosol and membrane fraction of a

Table 3
Primary antibodies used for specific protein quantification (slot blot, SB) and immunohistochemical localization (IHC) of ion transport proteins in gills of Atlantic cod (*G. morhua*). For validation of antibodies, see Fig. 1.

	Antibody	Description	Origin	Host	SB	IHC	Obtained by
A	Na^+/HCO_3^- co-transporter 1 (NBC1)	Designed against peptide sequence *EKEPFLGDKSFDK*, (3′ region)	Cod *(G. morhua)*	Rabbit	1:5000	1:50	Developed by Michael, K. & Lucassen, M. (*this study*)
B	$Na^+/K^+/Cl^-$ co-transporter 1 (NKCC1)	Designed against the C-terminus (MET-902 to SER-1212) of human colonic crypt, clone T4	Human	Mouse	1:200	1:50	Developmental Studies Hybridoma Bank, University of Iowa, Department of Biological Sciences, Iowa City, Iowa
C	Na^+/K^+ ATPase α (NKA)	Against chicken-α subunit (D. M. Fambrough, John Hopkins University, Baltimore, MD)	Chicken	Mouse	1:200	1:50	Developmental Studies Hybridoma Bank, University of Iowa, Department of Biological Sciences, Iowa City, Iowa
	Na^+/K^+ ATPase α (H300)	Corresponding to amino acids 551–850 mapping within an internal region of human Na^+/K^+-ATPase α1	Human	Rabbit		1:50	Santa Cruz Biotechnology, Inc. 2145 Delaware Avenue, Santa Cruz, CA, 95060 U.S.A.
D	Na^+/H^+-exchanger 2 (NHE2)	Designed against glutathione S-transferase fusion proteins incorporating the last 87 amino acid residues of NHE2; antibody 597 (Tse et al., 1994)	Human	Rabbit	1:1000	–	Kindly provided by Wilson. J.M., Department of Zoology, University of British Columbia, Vancouver, Canada V6T 1Z4
E	Na^+/H^+-exchanger 1 (NHE1)	C-terminus, clone 4E9, MBP fusion protein containing the entire C-terminal. hydrophylic domain of porcine NHE1	Pork	Mouse	1:500	–	Merck Millipore, Darmstadt, Germany
F	Na^+-dependent Cl^-/HCO_3^- antiporter (SLC26A6)	Designed against peptide sequence *RLKERSQRMNPSQIC*	Zebrafish *(D. rerio)*	Rabbit	1:500	–	Kindly provided by Hwang. P. P., Institute of Cellular and Organismic Biology, Academia Sinica, Nangang, Taipei, Taiwan, Republic of China (ROC)
G	V-type H^+ ATPase (VHA)	Designed against synthetic peptides corresponding to the subunit A region *(SYSKYTRALDEFYDK)*	Squid	Rabbit	1:500	–	Kindly provided by Tseng, Y.-C., Department of Life Science, National Taiwan Normal University, Taipei, Taiwan, Republic of China (ROC)

Table 4
Position and sequences of the outer and inner 3′ RACE-primers used for the elongation of the C-terminus sequence information of the GmNBC1 sequence fragment (*GO387248*).

DNA fragment	Primer ID	Term	Sequence
Outer PCR	Gm_NBC1_3R_F1	Forward	AAGTTCCTGGGTGTGAGAGAGC
	3′ OP (outer primer)*	Backward	GCGAGCACAGAATTAATACGACT*
	Gm_NBC1_F3	Forward	TCCATCGCTCACATCGACAGTC
	3′ OP (outer primer)*	Backward	GCGAGCACAGAATTAATACGACT*
Control PCR	Gm_NBC1_F3	Forward	TCCATCGCTCACATCGACAGTC
	Gm_NBC1_B25	Backward	TCGTCCTCCTTCCTCTTCTTGTCC
Inner PCR	Gm_NBC1_3R_F2	Forward	TGGGTCCTAAAGTCCACCGTTG
	3′ IP (inner primer)*	Backward	CGCGGATCCGAATTAATACGAC TCACTATAGG*
	Gm_NBC1_3R_F1	Forward	AAGTTCCTGGGTGTGAGAGAGC
	3′ IP (inner primer)*	Backward	CGCGGATCCGAATTAATACGAC TCACTATAGG*

* Provided by manufacturer.

randomly chosen cod (*G. morhua*) gill tissue sample were fractionated by SDS-PAGE on 12% polyacrylamide gels according to Laemmli (1970). Blotting was performed as described above using a tank blotting system (Bio-Rad, Munich, Germany). For validation of specificity of the cod NBC1 antibody, blots were incubated either with the pre-immune serum (1:5000) or the final bleeding serum (1:5000) after preincubation of the antibody with excess antigen (1.60 μg μl^{-1}) for 20 min at room temperature and compared to serum obtained from the final bleeding (Fig. 1). The molecular weight of a specific protein band of about ~130 kDa in the crude extract, which could be enriched in the membrane fraction compared to the cytosolic fraction, is in line with published values for full-length marine NBC1 (e.g. 119.8 kDa; *Z. viviparus*; EU552532), indicating the successful synthesis of a cod specific NBC1 antibody. Further details on all primary antibodies are given in Table 3 and in Fig. 1.

2.10. ATPase activity measurements

Activity of Na^+/K^+ ATPase was measured in crude gill tissue extracts (see Animals section for respective sampling design) in a coupled enzyme assay with pyruvate kinase (PK) and lactate dehydrogenase (LDH) modified after the method of Allen and Schwartz (1969) by adopting a microplate reader (Biotec Power Wave HT, BioTek Instruments GmbH, Bad Friedrichshall, Germany). Enzyme activity was determined at 10 and 18 °C assay temperature in each treatment group. Plates were pre-equilibrated to 10 °C and 18 °C in a temperature block (modified after Weiss et al. (2012)). After a pre-run time of 2 min, measurements were started in a row by adding the extracts, which were measured in quadruplicates. The decrease of extinction at 339 nm was read-out within 2 s at 10 succeeding time points over a period of 10 min. The specific ATPase activities were determined as the difference of total ATPase (TA) activity and inhibitor-insensitive activities (NA) using 5 mM ouabain for the Na^+/K^+ ATPase, 16 μM bafilomycin A1 for the H^+ ATPase and 60 μM oligomycin for the F_1F_o ATP synthase as inhibitors. Activities are given as micromoles of consumed ATP per g tissue fresh weight (fwt) and hour (μmol ATP g^{-1} fwt h^{-1}) at the respective acclimation temperature.

2.11. Protein localization

Gill arches of cod from the control group were fixed by direct immersion in Bouin's solution and immunohistochemistry on paraffin sections was performed as described by Hu et al. (2014). Primary antibodies were diluted 1:50 in PBS, placed in small droplets on the gill sections and were incubated overnight at 4 °C in a wet chamber. The procedure was repeated with the respective second primary antibodies. After washing with PBS, the respective secondary antibodies (anti-rabbit AlexaFlour 594/anti-mouse AlexaFlour 488, Invitrogen, Oregon, USA) were diluted 1:300 and incubated for 1 h at RT. After washing, sections were examined under Leica SP2/Leica SP5 confocal laser-scanning microscopes (Leica Microsystems, Wetzlar, Germany). Controls were performed without application of the first antibody using the same procedure. For NKCC1/NKA co-staining, the primary antibody for NKA α subunit was a H-300 rabbit polyclonal antibody, which was already successfully used for immunolocalization in fish (Lorin-Nebel et al., 2012; Riou et al., 2012). For details on primary antibodies see Table 3 and Fig. 1.

2.12. Data analysis and statistics

All values are expressed as means with standard error of the mean (SEM). Outliers were identified using the ROUT (robust regression followed by outlier identification) method (Q set to ≤10%) and removed. Remaining samples were tested for normal distribution (D'Agostino–Pearson omnibus normality test) and homogeneity of variances (Brown–Forsythe test). If appropriate, ordinary analyses of variance were applied (two-way ANOVAs) followed by Sidaks multiple comparison-test as post-hoc test. If normal distribution and/or homogeneity of variances were not given, data were transformed using a log (Y) transformation. If assumptions for parametric tests were still violated, one-way ANOVAs/Kruskal–Wallis non-parametric ANOVAs followed by Sidaks/Dunns multiple comparison test and multiple t-tests corrected for multiple comparisons (Sidak–Bonferroni method) were applied to test for differences between acclimation temperatures. Statistical significance was tested at the $p \leq 0.05$, $p \leq 0.01$ and $p \leq 0.001$ levels. Given p-values are corrected for multiple comparisons (adjusted p). In all cases, post-hoc tests only tested for significant differences between acclimation temperatures (10 °C or 18 °C) or PCO_2 levels. Different letters denote significant differences between PCO_2 treatments at 10 °C (a/b) and 18 °C (A/B), whereas a hash key indicates differences between acclimation temperatures at the respective PCO_2 level. All statistical analyses were performed using Graph Pad Prism Software version 6.0 (GraphPad Prism version 6.0 for Mac OS.X, GraphPad Software, La Jolla, California, USA). Spearman correlation analysis was performed using the *CCA* package in R and corresponding correlation matrices were used as input for correlation networks built by the *qgraph* package in R (Epskamp et al., 2012). For comparability of graphs, highest edge weight was set to 1. Only significant ($p \leq 0.05$) correlations were reported. For corresponding Spearman correlation coefficients, see supplementary material.

3. Results

3.1. Cellular localization of branchial ion transport proteins

Only antibodies against NKCC1, Na^+/K^+ ATPase α subunit (NKA) and the newly generated antibody against NBC1 were applicable in immunohistological analyses of gill sections from Atlantic cod reared under control conditions. The co-staining of NKCC1 and NKA (Fig. 2A) revealed a co-localization of both proteins in the interlamellar space as well as on the basal part of the secondary lamellae. NBC1 protein largely co-localized with NKA on the basal part of the secondary lamellae (Fig. 2B) as well as in the interlamellar space in the gill sections.

3.2. Transcriptional regulation of branchial ion transporters

A PCO_2-dose-dependent decrease of total gill tissue RNA content [μg mg fwt^{-1}] occurred in fish acclimated at optimum temperature, whereas a generally lower RNA content was found in the warm-acclimated groups at low and medium PCO_2 (Table 1). In addition, gene expression of individual branchial ion transporters revealed temperature-dependent responses to elevated PCO_2 (Fig. 3). Except for NBC1 and NHE2, mRNA levels of all ion transporters studied were generally lower in fish acclimated at 18 °C and control and medium

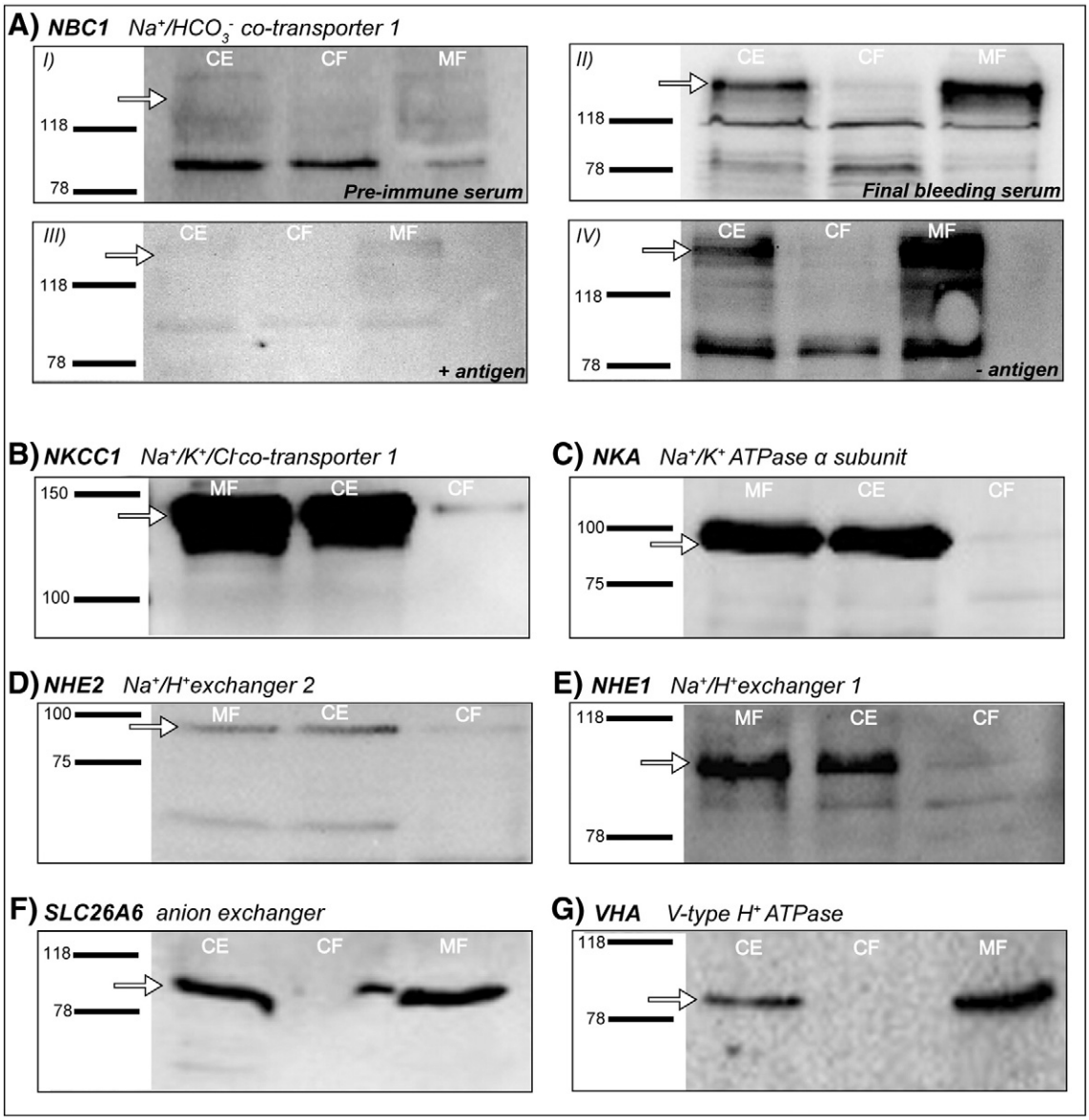

Fig. 1. Validation of antibody specificity in gills of Atlantic cod. Antibody specificity was validated in cod gill protein extracts (CE = crude extract, CF = cytosolic fraction, MF = membrane fraction) by Western blot. Protein standards used were pre-stained SDS-PAGE standard, broad range, Bio-Rad, Munich, Germany (for NHE1, SLC26A6, VHA and NBC1) and ECL DualVue Western Blotting Markers (GE Healthcare, UK) for NKA, NKCC1 and NHE2.

PCO_2 than in fish at 10 °C. In opposite, no decrease or even higher mRNA expression was generally found at 18 °C and high PCO_2.

At 10 °C acclimation temperature, mRNA expression of some ion transporters was significantly higher at medium PCO_2 than at low and high PCO_2: NHE1B mRNA expression increased nearly 10-fold at medium PCO_2 above mRNA levels found at low and high PCO_2 (Fig. 3D). Similarly, transcript levels of all three Na^+/K^+ ATPase α subunits (ATNA1, A2 and A3) increased at medium PCO_2 (Fig. 3H–J). In contrast, mRNA expression of the anion transporter SLC26A6 decreased nearly 2-fold under this treatment (Fig. 3B). A trend to lower mRNA expression at medium PCO_2 became obvious for NBC1 (Fig. 3A). NHE1A mRNA expression displayed a divergent response pattern, as transcript levels decreased nearly 4-fold in fish acclimated at high PCO_2 compared to low and medium PCO_2 (Fig. 3C).

The transcriptional response differed considerably in gills of warm acclimated fish. At high PCO_2, mRNA expression of H^+ ATPase subunit V1A (VHA–V1A; Fig. 3G) as well as of NKCC1 (Fig. 3F) increased nearly 2-fold compared to low and medium PCO_2. NHE1A transcript levels decreased ~8-fold at medium PCO_2 compared to low and high PCO_2 (Fig. 3C). Again, a trend to lower mRNA expression at medium PCO_2 became obvious for the NBC1 (Fig. 3A). The largest responses were observed for NHE1B and ATNA2 (Fig. 3D and I). Their transcript levels correlated positively with elevated PCO_2, increasing about 10-fold (NHE1B; Fig. 3D) and ~55-fold (ATNA2; Fig. 3I) from low to high PCO_2. It is important to note that NHE1B abundance was about 400-fold lower than NHE1A in cod gills. The difference was even larger for the Na^+/K^+ ATPase subunit A2, where the mean expression of ATNA2 was by a factor of 1000 lower than that of isoform ATNA1, which showed the highest cellular isoform abundance.

Correlation analysis on the mRNA expression profiles of individual ion transporters at both acclimation temperatures were used to detect co-regulations of specific transporters forced by elevated PCO_2 as driver. Thus, effects of PCO_2 hidden under the reasonable individual variation when analyzing gene expression separately may become visible. The correlation networks revealed a temperature-dependent regulatory relationship between the investigated transporters driven by PCO_2 (Fig. 4). At optimum temperature (Fig. 4A), Na^+/K^+ ATPase subunit expression profiles changed always in parallel. Furthermore, ATNA1 and

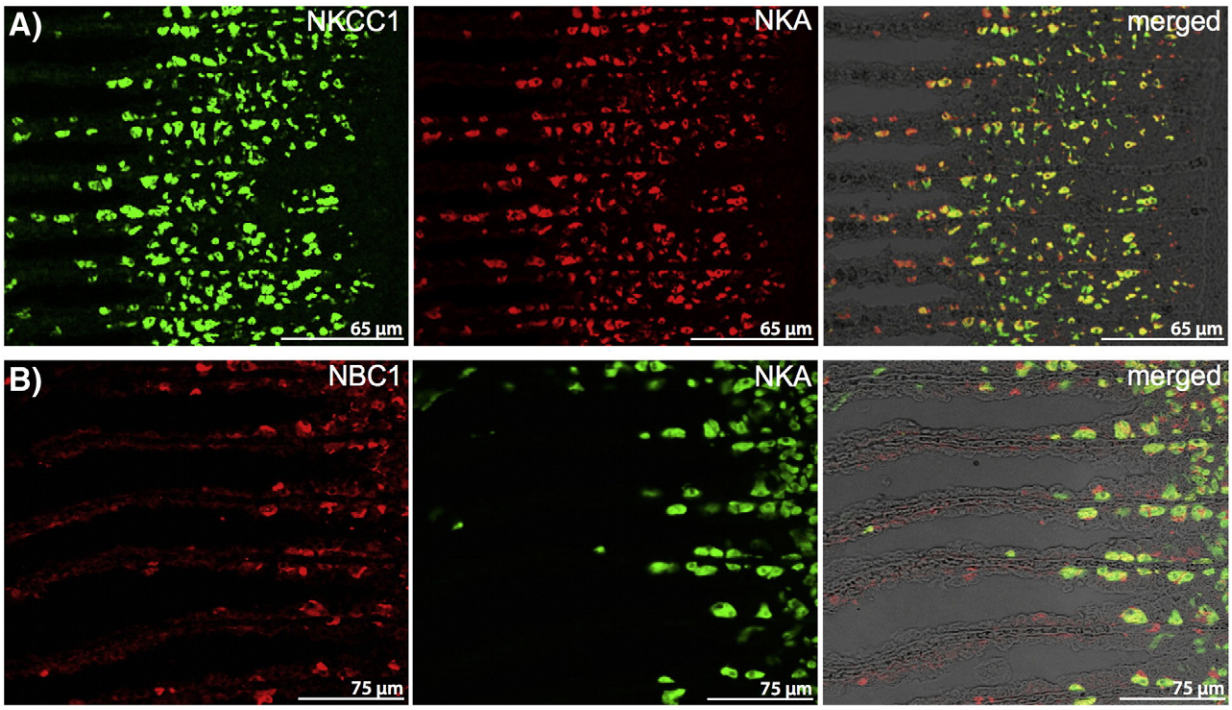

Fig. 2. Co-staining of NKCC1 and NBC1 with Na^+/K^+ ATPase (NKA). Co-staining of (A) NKCC1 ($Na^+/K^+/Cl^-$ co-transporter 1) and (B) NBC1 (Na^+/HCO_3^- co-transporter 1) with Na^+/K^+ ATPase (NKA) in gills of Atlantic cod (*G. morhua)* reared at control conditions (10 °C). Antibody specificity was validated by Western blots (see also Table 3; Fig. 1).

A3 formed a cluster with NKCC1, NHE2 and VHA–V1A, whereas the connection to Na^+/K^+ ATPase subunit A2 was weaker. NHE1B expression was only correlated with Na^+/K^+ ATPase subunits A2 and, to a lesser extent with A3. SLC26A6 was the only gene showing pronounced negative correlations with all Na^+/K^+ ATPase subunits, but was positively correlated with NBC1. At 18 °C (Fig. 4B), SLC26A6 became separated, as these correlations were not evident anymore. Instead, NBC1 together with NHE1A joined the cluster of ATNA1, ATNA3, NKCC1, NHE2 and VHA–V1A, which was already observed at 10 °C acclimation temperature. The low abundance transcripts ATNA2 and NHE1B (see above) were separated due to their pronounced responses in expression, while becoming correlated more tightly at the same time. In contrast, the expression profile of SLC26A6 only displayed weak and again, negative correlations.

3.3. Protein expression of branchial ion transporters

Similar gill tissue protein contents in all treatments indicate no general shift in protein expression (Table 1). At 10 °C acclimation temperature, specific protein expression of all ion transporters quantified by specific antibodies remained unchanged at all PCO_2 levels (Fig. 5). In contrast, warming to 18 °C caused NHE1, NHE2, VHA as well as NKCC1 protein expression to increase about 1.5-fold at medium PCO_2 compared to fish acclimated either at low or high PCO_2 or compared to both (Fig. 5C–E and G), leading to higher specific protein levels than in fish acclimated at 10 °C under this treatment. Protein expression of the two bicarbonate transporters (NBC1 and SLC26A6) revealed the same pattern, but changes remained statistically non-significant (Figs. 5A and 4B). The amount of NKA protein did not change between treatments (Fig. 5F). Although specific protein expression on average remained stable at 10 °C acclimation temperature, correlation analysis revealed a co-regulation of NKCC1, NHE1, NBC1 and NHE2 (Fig. 6A) protein expression levels, whereas VHA protein expression was only correlated with that of NKA and NHE1. In warm acclimated fish, protein expression levels of all transporters (NKCC1, NBC1, NHE2, NHE1 and VHA) except for NKA and SLC26A6 were highly correlated in response to elevated PCO_2 (Fig. 6B). Correlation between the overall responses of VHA and NKA expression was weak in warm acclimated fish.

3.4. Functional capacities of branchial ion transporting ATPases and F_1F_o ATP-synthase

Enzyme activities are presented at the respective acclimation temperature to illustrate in vivo conditions (Fig. 7). Na^+/K^+ ATPase activities were PCO_2 independent. However, at 18 °C acclimation and assay temperatures they were nearly 2-fold higher than at 10 °C, revealing an uncompensated rise of Na^+/K^+ ATPase capacities with habitat temperature (Fig. 7A). Na^+/K^+ ATPase Q10 values determined between 10 °C and 18 °C assay temperature ranged around 2 and were similar across treatments (see Table 5). Enzymatic capacity of H^+ ATPase was depressed by medium PCO_2 in fish acclimated at 10 °C, but remained unaffected by PCO_2 at 18 °C (Fig. 7B). No temperature effect was observed, indicating thermally compensated H^+ ATPase activities in the warmth. However, H^+ ATPase Q10 values in warm acclimated fish were significantly lower at medium than at high PCO_2 as well as compared to fish acclimated at 10 °C, indicating a reduced, but PCO_2-dependent temperature sensitivity of H^+ ATPase in warm acclimated fish (see Table 5). F_1F_o ATP-synthase capacities were independent of PCO_2 and remained uncompensated at warm temperatures (Fig. 7C), mirrored in significant increments (~2-fold) at 18 °C acclimation temperature at medium and high PCO_2. Similar to Na^+/K^+ ATPase, Q10 values of F_1F_o ATP-synthase (~2; see Table 5) remained unchanged across treatments. The capacities of the two ATP-demanding ion pumps (Na^+/K^+ ATPase and H^+ ATPase) were correlated with the capacities of ATP-producing mitochondrial F_1F_o ATP-synthase at both acclimation temperatures. The strongest correlation was found between Na^+/K^+ ATPase and F_1F_o ATP-synthase (Fig. 7D; $p < 0.0001$) at both temperatures, the correlations between H^+ ATPase and F_1F_o ATP-synthase (Fig. 7E) and between H^+ ATPase and Na^+/K^+ ATPase (Fig. 7F) were less pronounced ($p \leq 0.01$).

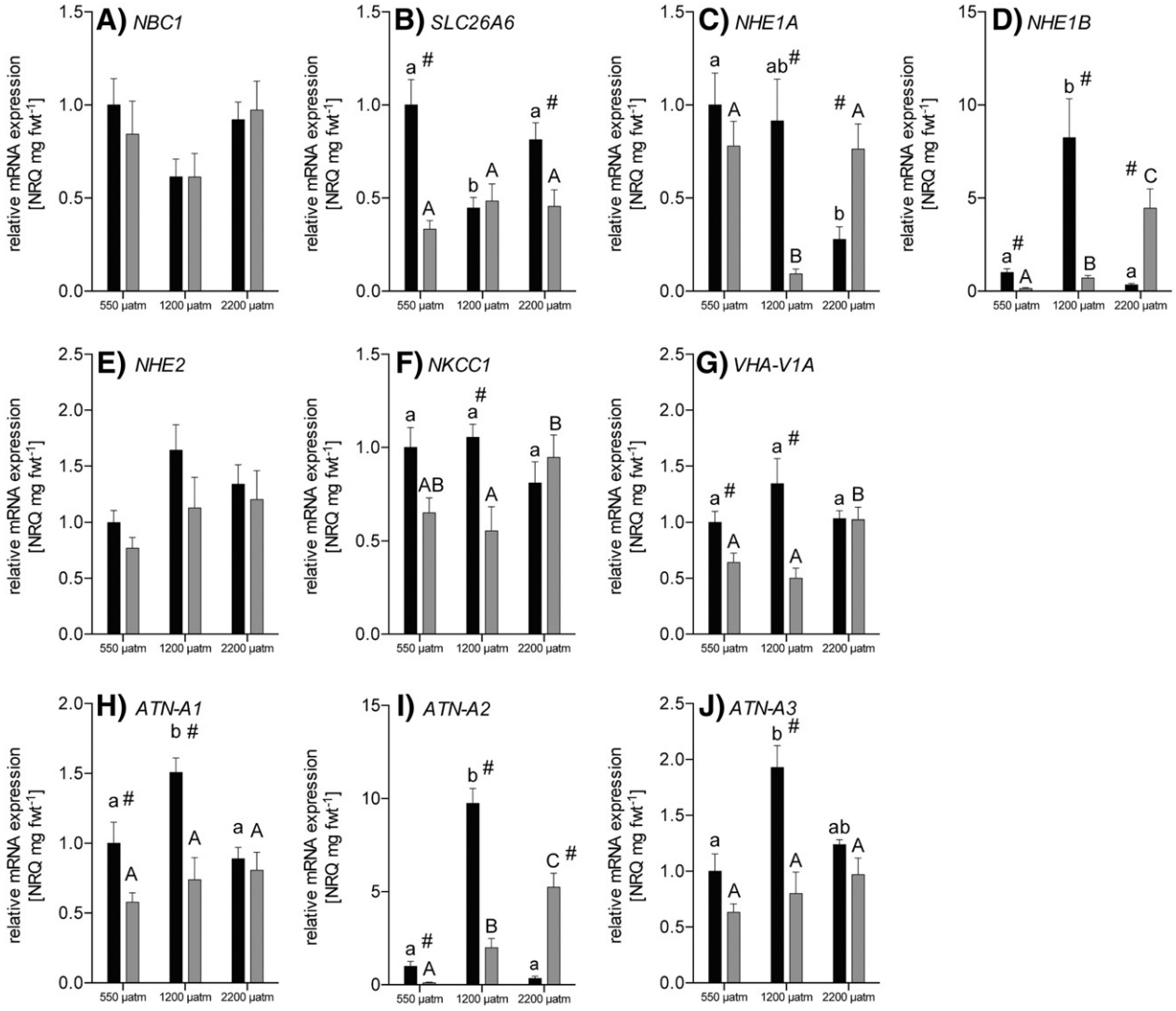

Fig. 3. Ion transporter mRNA expression in gills of Atlantic cod. mRNA expression of ion transporters (NRQ mg fwt^{-1}; fractional values relative to those found at 10 °C in the low PCO_2 treatment) in gills of Atlantic cod (*G. morhua*) acclimated to 550 µatm, 1200 µatm and 2200 µatm CO_2 and 10 °C (black bars) or 18 °C (gray bars), respectively. mRNA expression levels were normalized to the expression of the reference genes UBI and RPL22. Post-hoc tests only tested for significant differences within acclimation temperatures and PCO_2 levels. Different letters denote significant differences between PCO_2 treatments at 10 °C (a/b) and 18 °C (A/B), whereas a hash key indicates differences between acclimation temperatures at 550 µatm, 1200 µatm and 2200 µatm, respectively. n = 7–10 per treatment. Values are depicted as means ± SEM.

4. Discussion

With a few notable exceptions, most studies of ion and acid base regulation in marine fish were conducted using very high PCO_2 levels and only monitored the initial compensatory phase. Here, the combined effects of elevated temperature and moderately elevated PCO_2 on gene and protein expression as well as on functional capacities of important ion transporters were determined in gills of a marine fish after long-term acclimation over 4 weeks.

4.1. Transcriptional regulation of branchial ion transporters

Transcriptional regulation of branchial ion transporters revealed a temperature-dependent response to elevated PCO_2 (Fig. 3). Generally, total RNA content and transcript levels of ion transporters were lower in gills of warm acclimated fish than at 10 °C at control and medium PCO_2 (Fig. 3 and Table 1). This can be attributed to warm compensated transcription and, as total RNA content mainly represents ribosomal RNA, translational capacities, resulting in unchanged total protein content between acclimation temperatures (Table 1). However, no difference or even higher transcript levels were observed at high PCO_2 (Fig. 3) due to the PCO_2-dependent decrease of total RNA content in fish acclimated at optimum temperature, which was not found in warm acclimated fish (Table 1). These findings indicate that the branchial RNA synthesis machinery as well as translational capacities might be negatively affected by elevated PCO_2 at optimum temperature, whereas this effect was compensated for in the warmth, possibly by the stimulation of translation. Accordingly, the oxygen demand allocated to RNA and protein synthesis was found to be lower in gills of Atlantic cod in response to long-term acclimation at 2500 µatm and 10 °C, compared to fish acclimated at 18 °C (Kreiss et al., 2015a). As total protein content remained unchanged (Table 1), the PCO_2 induced reduction in translational capacities in gills of cod acclimated at 10 °C may be possibly compensated for by increased ribosomal efficiency or reduced protein degradation.

The pronounced increase in mRNA expression of all three Na^+/K^+ ATPase α subunits (ATNA1, A2 and A3, Fig. 3H–J) at medium PCO_2 and 10 °C indicates a tightly co-regulated response at transcriptional level to PCO_2 at optimum temperature. However, the magnitude of the response differed between subunits. Compared to ATNA1 and A3, which increased by a factor of 1.5–2, ATNA2 mRNA expression increased about 10-fold above control levels at medium PCO_2 and optimum

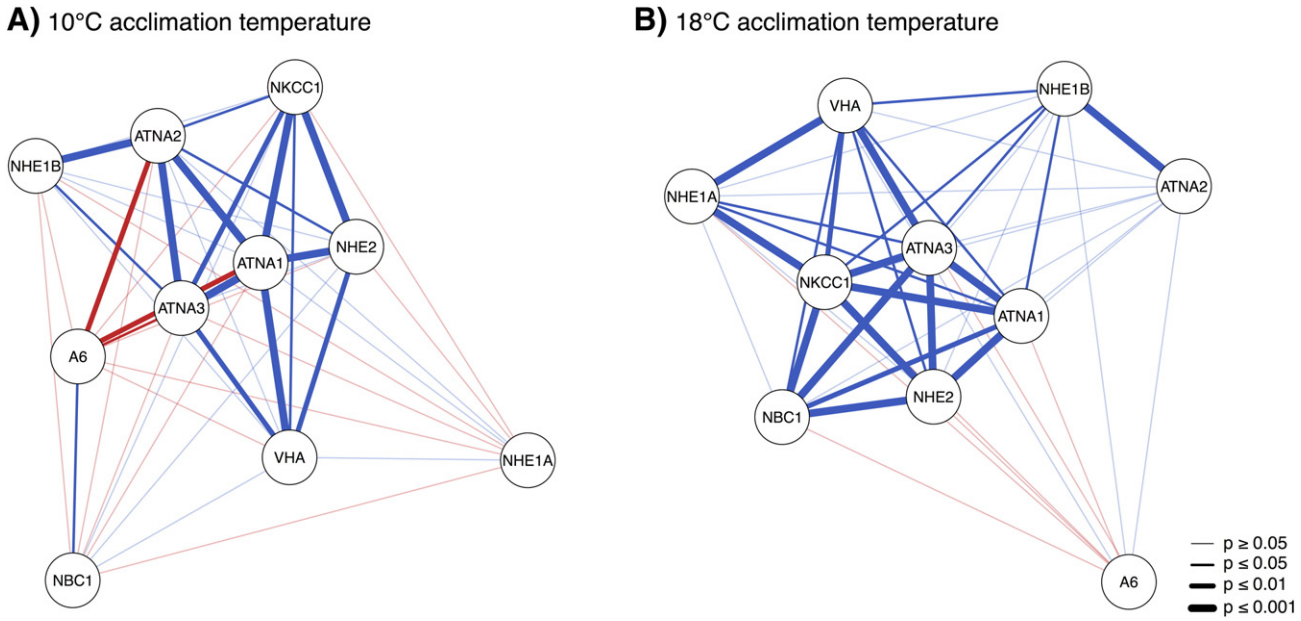

Fig. 4. Correlation networks of ion transporter mRNA expression. Correlation networks of ion transporter mRNA expression in gills of Atlantic cod (*G. morhua*) acclimated to 550 μatm, 1200 μatm and 2200 μatm CO_2 and 10 °C (A) or 18 °C (B), respectively. Spearman correlation analysis was performed and the corresponding matrices were used as input for correlation networks. Edge width was scaled according to respective significance levels (0.05, 0.01 and 0.001). Color saturation was cut at $p \geq 0.05$. For corresponding Spearman correlation coefficients, see supplementary material.

temperature. In warm acclimated fish the response of ATNA2 mRNA to PCO_2 differed even more, as ATNA2 increased dose-dependently by a factor of 55 between control and high PCO_2, whereas the expression of ATNA1 and A3 remained unaffected by PCO_2. These findings may be related to the generally 1000-fold lower transcript abundance of this isoform in cod gills, indicating that ATNA2 is an inducible isoform, which is only expressed under certain conditions.

The differential responses of mRNA expression of all Na^+/K^+ ATPase α subunits were further emphasized by the structure of the correlation networks (Fig. 4). In contrast to ATNA2, ATNA1 and A3 mRNA

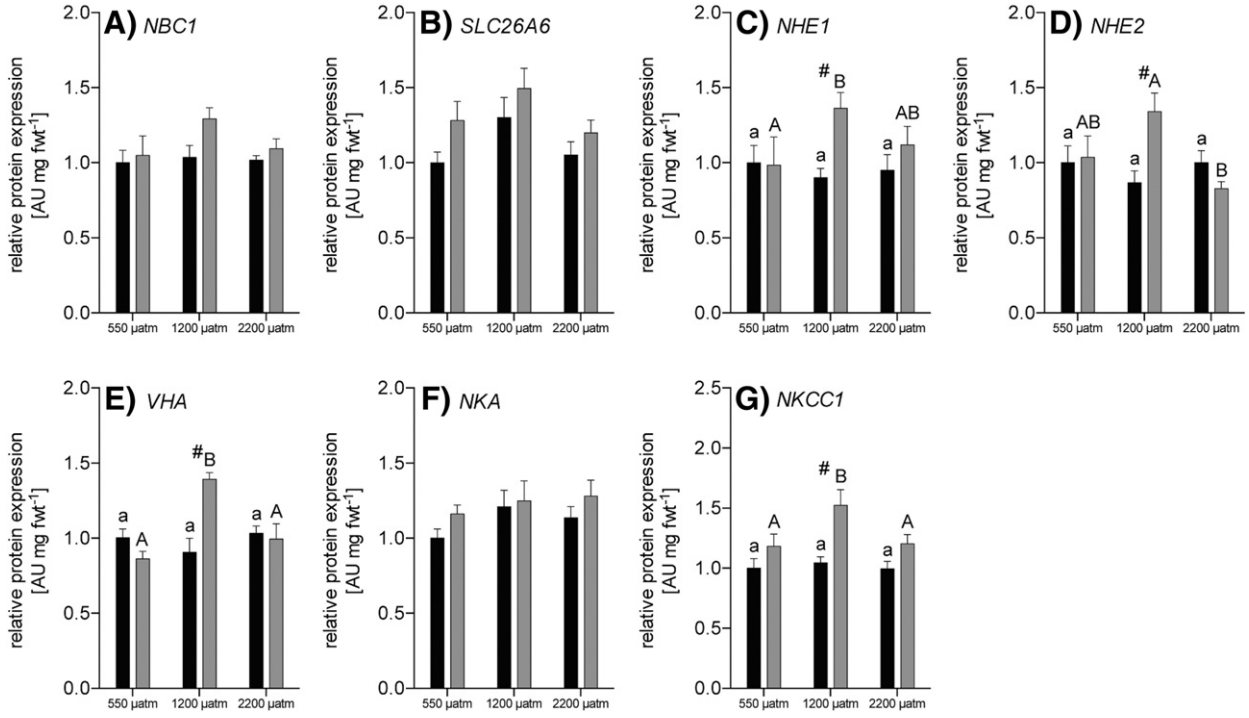

Fig. 5. Ion transporter protein expression in gills of Atlantic cod. Ion transporter protein expression [AU mg fwt^{-1}; fractional values relative to those found at 10 °C in the low PCO_2 treatment] in gills of Atlantic cod (*G. morhua*) acclimated to 550 μatm, 1200 μatm and 2200 μatm CO_2 and 10 °C (black bars) or 18 °C (gray bars), respectively. Protein concentrations were recalculated from calibration curves. Post-hoc tests only tested for significant differences within acclimation temperatures and PCO_2 levels. Different letters denote significant differences between PCO_2 treatments at 10 °C (a/b) and 18 °C (A/B), whereas a hash key indicates differences between acclimation temperatures at 550 μatm, 1200 μatm and 2200 μatm, respectively. n = 7–10 per treatment. Values are depicted as means ± SEM.

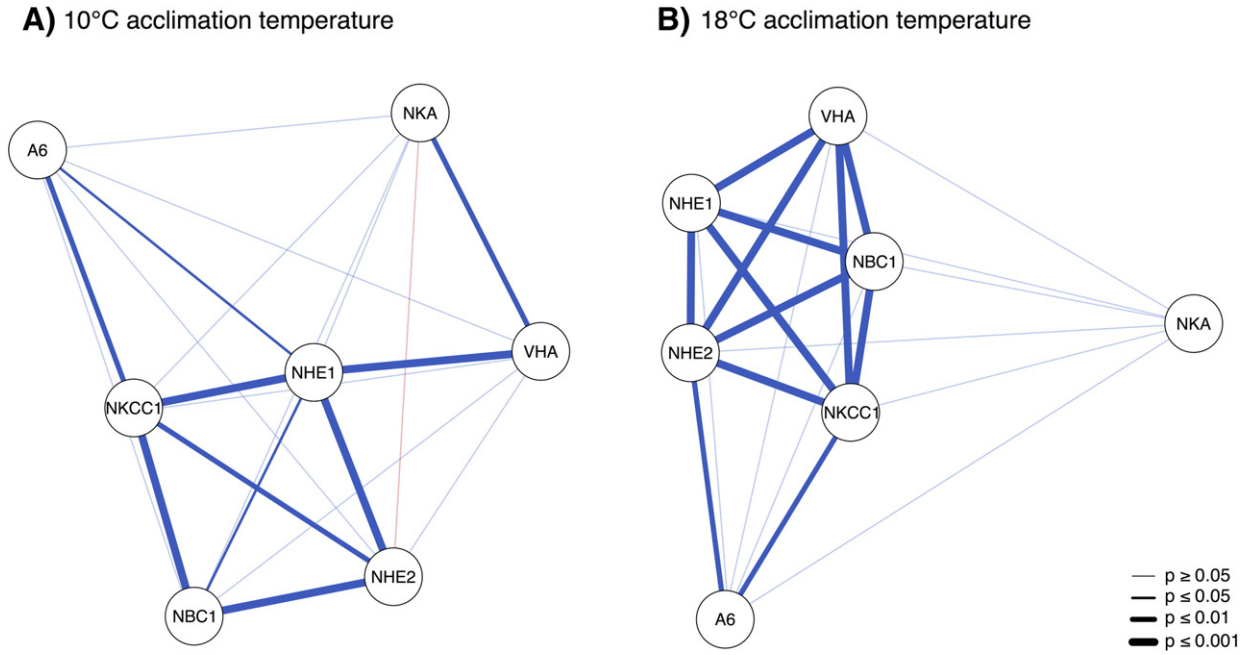

Fig. 6. Correlation networks of ion transporter protein expression. Correlation networks of ion transporter protein expression in gills of Atlantic cod (*G. morhua*) acclimated to 550 μatm, 1200 μatm and 2200 μatm CO_2 and 10 °C (A) or 18 °C (B), respectively. Spearman correlation analysis was performed and the corresponding matrices were used as input for correlation networks. Edge width was scaled according to respective significance levels (0.05, 0.01 and 0.001). Color saturation was cut at p ≥ 0.05. For corresponding Spearman correlation coefficients, see supplementary material.

expression were correlated with NKCC1, NHE2 and VHA mRNA expression at both acclimation temperatures, constituting a functional cluster with these ion transport proteins. ATNA2 mRNA expression reflected a different regulation pattern, which was even more pronounced at 18 °C (Fig. 4B). The correlated response of Na^+/K^+ ATPase subunits ATNA1 and A3 with NKCC1 mRNA expression to PCO_2 at both acclimation temperatures emphasizes the functional relationship of these transporters, both highly involved in branchial NaCl export in marine

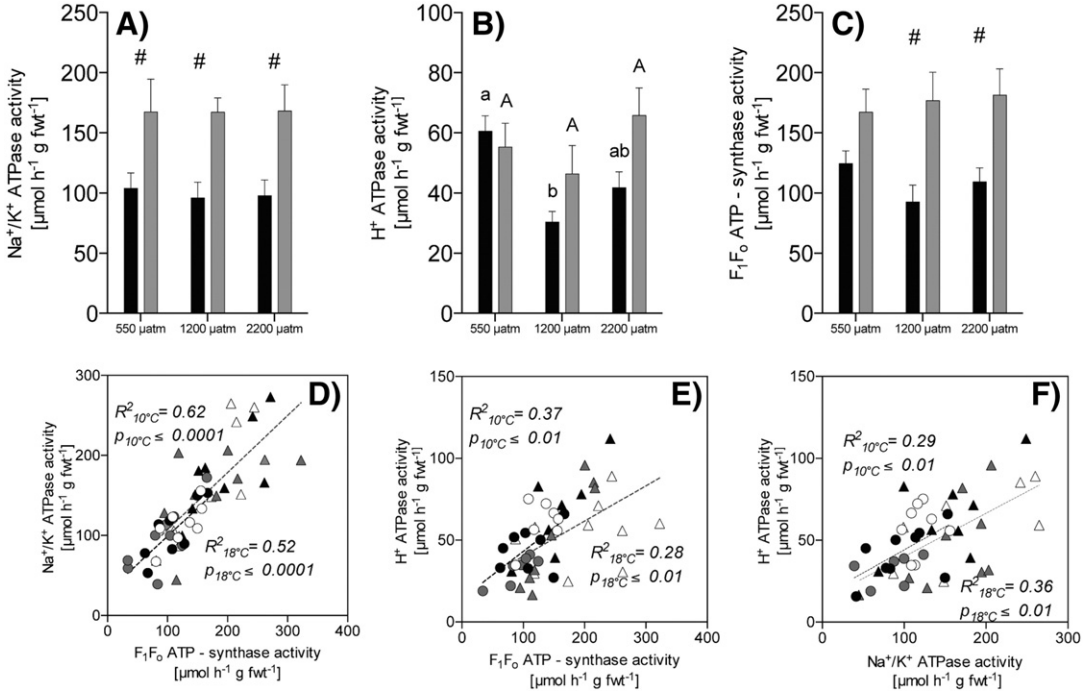

Fig. 7. Capacities of branchial Na^+/K^+ ATPase, H^+ ATPase and F_1F_o ATP-synthase. Capacities of (A) Na^+/K^+ ATPase, (B) H^+ ATPase and (C) F_1F_o ATP-synthase [μmol g fwt^{-1} h^{-1}]; (D) correlation of F_1F_o ATP-synthase capacity with Na^+/K^+ ATPase, (E) F_1F_o ATP-synthase capacity with H^+ ATPase capacities and (F) correlation of Na^+/K^+ ATPase capacity with H^+ ATPase capacities determined at the respective acclimation temperature in gills of Atlantic cod (*G. morhua*) acclimated to 550 μatm (white symbols), 1200 μatm (gray symbols) and 2200 μatm (black symbols) CO_2 and 10 °C (black bars; circles) or 18 °C (gray bars; triangles), respectively. Post-hoc tests only tested for significant differences within acclimation temperatures and PCO_2 levels. Different letters denote significant differences between PCO_2 treatments at 10 °C (a/b) and 18 °C (A/B), whereas a hash key indicates differences between acclimation temperatures at 550 μatm, 1200 μatm and 2200 μatm, respectively. For (D–F), significance was tested within acclimation temperatures, indicated by the respective R^2 and p-values in the graph. n = 7–10 per treatment. Values are depicted as means ± SEM.

Table 5
Branchial ATPase (Na^+/K^+ ATPase and H^+ ATPase) and F_1F_o ATP-synthase Q10 values in gill tissue of Atlantic cod (*G. morhua*) acclimated to 550 μatm, 1200 μatm and 2200 μatm CO_2 at 10 °C or 18 °C. Enzyme activities were determined at 10 °C and 18 °C assay temperature, respectively. n = 7–10 per treatment. Values are depicted as means ± SEM.

		Na^+/K^+ ATPase	V-type H^+ ATPase	F_1F_o ATP-synthase
10 °C	550 μatm	1.52 ± 0.20	1.58 ± 0.26	1.62 ± 0.17
	1200 μatm	1.86 ± 0.32	2.76 ± 0.39	1.79 ± 0.17
	2200 μatm	1.93 ± 0.20	1.54 ± 0.09	2.04 ± 0.16
18 °C	550 μatm	1.61 ± 0.34	1.81 ± 0.49^{AB}	2.18 ± 0.35
	1200 μatm	2.22 ± 0.30	$0.94 \pm 0.22^{A\#}$	1.88 ± 0.20
	2200 μatm	2.22 ± 0.18	2.51 ± 0.52^{B}	2.70 ± 0.30

fish (Evans et al., 2005; Marshall and Grosell, 2006; Hwang et al., 2011; Hiroi and McCormick, 2012). NKCC1 was found in basolateral membranes of ionocytes alongside with Na^+/K^+ ATPase (Pelis et al., 2001; Hiroi and McCormick, 2007; Tipsmark et al., 2008; Kang et al., 2011), which could also be confirmed for cod (Fig. 2A). To date, changes in NKCC1 mRNA expression were only found during salinity shifts and Parr–Smolt transformation (Cutler and Cramb, 2002; Tipsmark et al., 2002; Watson et al., 2014) but nothing is known about the role of branchial NKCC1 in response to hypercapnic conditions. Here, NKCC1 mRNA expression remained unchanged regardless of PCO_2 at optimum temperature, whereas at 18 °C, an increase of NKCC1 transcript levels was observed at high PCO_2. Therefore, transcriptional regulation of this transporter might be synchronized to the regulation of Na^+/K^+ ATPase capacities via α subunit transcripts as already observed for salmonids (Tipsmark et al., 2002), supporting NaCl homeostasis. Furthermore, the correlation of Na^+/K^+ ATPase and NKCC1 transcript levels with NHE2 mRNA expression driven by PCO_2 at both acclimation temperatures (Fig. 4) indicates a close co-regulation of NaCl homeostasis and Na^+ mediated proton export capacities via NHE2 at the apical side (Fig. 3E), thereby contributing to the reduction of the acid load.

The contribution of branchial proton excretion mechanisms like H^+ ATPase as well as the NHE isoform 1 to fish acid–base regulation is not yet clear for marine fish. A trend to lower H^+ ATPase mRNA expression was observed in gills of Japanese medaka (*Oryzias latipes*) in response to short term exposure to $PCO_2 \geq 7000$ μatm (Tseng et al., 2013). Similarly, NHE1 mRNA expression was found downregulated in several marine fish under acute exposure to severely hypercapnic conditions (Deigweiher et al., 2008; Rimoldi et al., 2009). Both transport proteins were assumed to be located basolateral in marine fish gill cells (Claiborne et al., 1999; Catches et al., 2006). Therefore, downregulated capacities would indicate decreased rates of proton excretion into the plasma, thereby possibly increasing the efficiency of systemic net acid excretion. However, after long-term acclimation, transcript levels of H^+ ATPase subunit V1A remained almost stable and even increased at high PCO_2 in warm acclimated cod (Fig. 3G). Thus, differences exist between the short-term and long-term response of the transcriptional regulation of H^+ ATPase to elevated PCO_2. Two NHE isoforms (NHE1A and 1B), which both belong to the NHE1 family and can be clearly separated from NHE2 according to sequence homology, were expressed in the gills of cod. The isoforms responded differentially to elevated PCO_2 and temperature. At 10 °C, NHE1A mRNA expression decreased ~4-fold at high PCO_2 compared to control, whereas at 18 °C, transcript levels were nearly 10-fold lower at medium PCO_2 (Fig. 3C), indicating decreased basolateral H^+ export capacities by this isoform under these treatments. NHE1B mRNA expression responded differently, increasing nearly 10-fold at medium PCO_2 and 10 °C, whereas transcript levels increased in a dose-dependent fashion at 18 °C (Fig. 3D). These differences between the regulation patterns of both isoforms may be attributed to their highly different expression levels, which was about 400-fold lower for NHE1B compared to NHE1A transcripts. According to this, about 10-fold higher mRNA expression levels of isoform NHE1A compared to NHE1B was found in eelpout gills (Deigweiher et al., 2008), indicating an inducible, supportive role of NHE1B to marine fish branchial acid–base regulation and a rather constitutive role for the later. The differential response of these two isoforms was also mirrored in correlation analysis (Fig. 4). Compared to NHE1A, the response of NHE1B was closely correlated with that of Na^+/K^+ ATPase subunit A2, both present at comparatively low levels under control conditions, but highly responsive to hypercapnia and temperature. Thus, both isoforms seem to be necessary only under certain conditions and/or in specific cell types.

Teleost fish pH compensation does not only involve net acid secretion. Under hypercapnic conditions, a direct or indirect net accumulation of bicarbonate, accompanied by an equimolar loss of anions was observed and proposed to be even more important (Toews et al., 1983; Larsen et al., 1997; Deigweiher et al., 2008; Esbaugh et al., 2012). The two members of bicarbonate transporter families investigated here (SLC26A6 and NBC1) both were suggested to transport HCO_3^- across the gill epithelium, either on the apical side in exchange for Cl^- (transporter family SLC26; Boyle et al., 2015; Perry et al., 2009; Piermarini et al., 2002) or basolaterally into the plasma (transporter family SLC4, NBC1; Deigweiher et al., 2008; Esbaugh et al., 2012; Hirata et al., 2003). SLC26A6 mRNA expression remained unchanged in toadfish gills (*Opsanus beta)* during acute exposure to 1900 μatm (Esbaugh et al., 2012). Here, mRNA expression of SLC26A6 decreased in response to medium PCO_2 at 10 °C (Fig. 3B), whereas it remained unchanged in warm acclimated fish. A trend to decreased transcript levels was also observed for NBC1 mRNA expression at medium PCO_2, regardless of acclimation temperature (Fig. 3A). However, some kind of response of NBC1 mRNA expression to PCO_2 is supported by the strong correlations to mRNA expression of the other transporters at warm temperatures (Fig. 4B). So far, NBC1 mRNA expression was found upregulated in gills of both, freshwater fish after exposure to acute (Perry et al., 2003) and in seawater fish after exposure to long-term (Deigweiher et al., 2008) severely hypercapnic conditions (≥10,000 μatm). Furthermore, an isoform-specific up- or downregulation of NBC1 mRNA expression was observed in gills of Japanese medaka (*O. latipes*) in response to short term exposure to $PCO_2 \geq 7000$ μatm (Tseng et al., 2013). In contrast, during acute exposure to 1900 μatm it remained unchanged (Esbaugh et al., 2012). Therefore, a dose-dependent as well as isoform-specific regulation pattern has to be anticipated for NBC1. The expression profiles of both bicarbonate transporters were tightly correlated only at 10 °C acclimation temperature (Fig. 4A). Together, both bicarbonate transporters may constitute a downregulation of apical HCO_3^- export via SLC26A6 at medium PCO_2 and 10 °C, simultaneously decreasing basolateral HCO_3^- import into the cell if NBC1 is functioning in the influx mode (Perry et al., 2003; Evans et al., 2005). Besides, both transporters may also be located in different cell types. In the Atlantic stingray (*Dasyatis sabina*), another member of the SLC26 family (pendrin, SLC26A4) was clearly located in H^+ ATPase rich cells and not in Na^+/K^+ ATPase rich cells (Piermarini et al., 2002). In cod, NBC1 is co-localized with Na^+/K^+ ATPase (Fig. 2B), implying that SLC26A6 and NBC1 might be located in different gill cell types. Shifting correlations of SLC26A6 and NBC1 between both temperatures (Fig. 4) may support this view. Further studies are needed to clearly define the cellular co-localization of both transporters in marine teleost fish.

4.2. Effects on protein expression of branchial ion transporters

The differential regulation observed on transcriptional level indicates a necessity for coordinated adjustments of cod branchial ion transport components in response to elevated PCO_2 and temperature. This translates to protein level, as the response of NKCC1, NBC1, NHE1 and NHE2 protein was tightly co-regulated at 10 °C and 18 °C (Fig. 6), despite the differences in protein expression between acclimation temperatures (Fig. 5). Again, this emphasizes the importance of regulating systemic acid–base status as well as NaCl homeostasis at the same time, supported by stable Na^+/K^+ ATPase protein quantities, which

remained unaffected by PCO_2 (Fig. 5F). Furthermore, no temperature effect on Na^+/K^+ ATPase protein expression was observed, indicating uncompensated protein quantities in response to warm acclimation. As the Na^+/K^+ ATPase antibody used here might not have the same affinity to all α subunits, specific shifts of α subunit expression could have taken place as reported upon salinity transfers (Lee et al., 1998; Richards et al., 2003; Madsen et al., 2008; Tipsmark et al., 2011), although the summed protein signal remained unchanged. However, the positive correlations between mRNA expression profiles of Na^+/K^+ ATPase α subunits at both acclimation temperatures exclude simple isoform switching in response to elevated PCO_2 and therefore, may rather indicate mutually supportive regulation pathways of stable protein expression.

Some functional relationships observed at the transcriptional level were translated to protein level and especially pronounced in warm acclimated fish as observed for protein as well as mRNA expression of NKCC1, NBC1, NHE2 and VHA (Figs. 4 and 6). Furthermore, protein expression of VHA and NHE1 increased at medium PCO_2 in warm acclimated fish (Fig. 5C and E), tightly correlated on transcriptional (NHE1A; Fig. 4B) as well as on protein level (Fig. 6B). These findings indicate a tightened co-regulation on both functional levels and thus, a functional relationship of these ion transport components under exposure to elevated PCO_2 and temperature. Similarly, NKCC1 and NHE2 protein expression levels were changing in a correlated fashion in response to changing acclimation temperatures and PCO_2 as already observed at transcriptional level, once again emphasizing an importance to coordinate apical Na^+/H^+ exchange with the regulation of NaCl homeostasis.

Our data provide evidence of a temperature-dependent increase of mRNA and protein expression of several ion transport proteins at medium PCO_2. As the fish were exposed to experimental conditions for four weeks, an acute upregulation of transporter specific mRNA and protein expression is unlikely, as compensation for acid–base disturbances during initial compensation is achieved within the first 24 h of exposure (Toews et al., 1983; Larsen et al., 1997; Esbaugh et al., 2012). However, the stronger responses of ion transport capacities observed at 1200 μatm compared to higher PCO_2 levels suggest a PCO_2-dependent compensatory response. Accordingly, the correlated increase of NHE2, NKCC1, VHA and NHE1 protein expression at 18 °C and medium PCO_2 (Fig. 5 and 6B) may imply higher requirements on branchial ion and acid–base regulation under this treatment. However, increased in vivo O_2 demand for branchial ion regulation through Na^+/H^+-exchange and HCO_3^- transport at 18 °C and high PCO_2 rather suggests a post-translational exploitation of existing transport capacities compared to medium PCO_2 (Kreiss et al., 2015b). Such a functional shift would match the observed tight co-regulation of ion transport components, especially at protein level in gills of warm acclimated fish (Fig. 6B).

4.3. Regulation of branchial ATPase capacities

Functional capacities of Na^+/K^+ ATPase remained unaffected by PCO_2 up to 2200 μatm (Fig. 7A). In previous studies (Esbaugh et al., 2012; Kreiss et al., 2015a) branchial Na^+/K^+ ATPase capacities were either found reduced or also unchanged under PCO_2 values ≤3000 μatm, whereas at PCO_2 ≥ 3000 μatm, increased functional capacities were observed (Deigweiher et al., 2008; Melzner et al., 2009a; Hayashi et al., 2013). Reduced Na^+/K^+ ATPase related oxygen consumption was found in isolated gill arches of cod acclimated at optimum temperature and moderately elevated PCO_2. In contrast, maximum capacities were maintained in vitro (Kreiss et al., 2015a), indicating variable exploitation of excess branchial Na^+/K^+ ATPase capacities in vivo. The stimulated functional capacities of Na^+/K^+ ATPase at 18 °C acclimation temperature (Fig. 7A) could be attributed to non-compensated protein quantities (Fig. 5F). Similarly, net O_2 demand of Na^+/K^+ ATPase was increased in isolated gill arches of Atlantic cod in vivo upon warm acclimation (Kreiss et al., 2015b), indicating elevated energy demand in support of ion homeostasis at temperatures close to summer maxima. In contrast, functional capacities of branchial H^+ ATPase were thermally compensated (i.e. down-regulated, when measured at a common assay temperature) in cod acclimated at 18 °C (Fig. 7B). Furthermore, hypercapnia reduced the capacity of the H^+ pump at optimum temperature and medium PCO_2. As VHA protein levels remained unchanged, the lower functional capacities observed in vitro has to originate from post-translational modifications. In warm acclimated fish, H^+ ATPase capacities remained PCO_2-independent but the lower Q10 value observed at medium PCO_2 (Table 5) despite increased H^+ ATPase protein expression (Fig. 5E) also indicates post-translational regulation.

Localization of the two most important branchial ATPases (Na^+/K^+ ATPase and H^+ ATPase) in mitochondria rich gill cells (ionocytes; see e.g. Hwang et al. (2011) for review) mirrors their coordination with cellular ATP producing capacities. Functional capacities of F_1F_o ATP-synthase were closely correlated with Na^+/K^+ ATPase and, to a lesser extent, with H^+ ATPase capacities (Fig. 7D and E). Therefore, branchial aerobic ATP supply was closely coordinated with ATP demanding components of ion and acid–base regulation under all treatments. However, variability increased in gills of warm acclimated fish. Furthermore, Na^+/K^+ ATPase protein expression was correlated to VHA protein levels at 10 °C acclimation temperature only (Fig. 6A), indicating closely coupled protein quantities and thus, functional coordination of branchial ATPases at optimum temperature. This was not evident in warm acclimated fish (Fig. 6B), possibly indicating the onset of thermally induced imbalances in the coordinated regulation and function of branchial ATPases.

5. Conclusions

In the present study, regulation patterns of important components of cod ion and pH homeostasis were compared at different functional levels to decipher essential mechanisms and combined effects of temperature and PCO_2. The differential regulation on transcriptional level supported stable protein levels at 10 °C, whereas protein expression of most transporters increased at medium PCO_2 in warm acclimated fish. Tightly co-regulated mRNA and protein expression of distinct ion transport proteins substantiate their functional relationships and indicate the importance of coordinated regulation of transport components involved in systemic acid–base as well as ion regulation in response to elevated PCO_2. Warming increased the connections between most transporters, which may indicate a higher selective pressure for coordinated interaction between the different processes in response to elevated PCO_2. However, weakened correlation of NKA to the other ion transporters would indicate some loss of coordination between the main ion-motive component and secondary ion transport processes in the gills.

In line with the localization of branchial ATPases in mitochondria rich gill cells, functional capacities of F_1F_o ATP-synthase co-varied and were thus generally correlated with Na^+/K^+ ATPase and H^+ ATPase capacities. These regulatory patterns indicate physiological plasticity in the gills of cod to adjust to a warming, acidifying ocean, but interacting and non-linear, dose-dependent effects of both climate factors have to be considered. Increasing variability in the correlation of branchial ATP demand and supply, a tightened co-regulation of ion transport components as well as uncompensated Na^+/K^+ ATPase capacities became obvious in gills of warm acclimated fish, suggesting that elevated temperature might become a limiting factor for ion and acid–base regulation when rising above summer maxima (18 °C). How these patterns support the ability of cod to adapt to a future ocean remains to be explored.

Acknowledgments

The authors would like to thank Bengt Lundve, Lars Ljungqvist and the whole staff of the Sven Lovén Centre for Marine Sciences in Kristineberg, Sweden for obtaining experimental animals and valuable technical support and Karim Zanaty for conducting enzyme activity

measurements at the Alfred Wegener Institute, Helmholtz Center for Polar and Marine Research (AWI). Stephan Frickenhaus (AWI) is gratefully acknowledged for substantial support and input on bioinformatics. This work was funded by the joint project BIOACID (Biological Impacts of Ocean Acidification, phase 1; FKZ 03F0608B, sub-project 2.3.2) of the German Federal Ministry of Education and Research (BMBF) and a contribution to the PACES research program (work package 1.6) of the AWI funded by the Helmholtz Association. Sam Dupont is funded by the CeMEB (cemeb.science.gu.se) and supported by a Linnaeus grant from the Swedish Research Council and Formas.

Appendix A. Supplementary data

Supplementary data to this article can be found online at http://dx.doi.org/10.1016/j.cbpb.2015.12.006.

References

Allen, J.C., Schwartz, A., 1969. A possible biochemical explanation for the insensitivity of the rat to cardiac glycosides. J. Pharmacol. Exp. Ther. 168, 42–46.

Andersen, C.L., Jensen, J.L., Ørntoft, T.F., 2004. Normalization of real-time quantitative reverse transcription-PCR data: a model-based variance estimation approach to identify genes suited for normalization, applied to bladder and colon cancer data sets. Cancer Res. 64, 5245–5250. http://dx.doi.org/10.1158/0008-5472.CAN-04-0496.

Boyle, D., Clifford, A.M., Orr, E., Chamot, D., Goss, G.G., 2015. Mechanisms of Cl^- uptake in rainbow trout: cloning and expression of slc26a6, a prospective Cl^-/HCO_3^- exchanger. Comp. Biochem. Physiol. A Mol. Integr. Physiol. 180, 43–50. http://dx.doi.org/10.1016/j.cbpa.2014.11.001.

Bradford, M.M., 1976. A rapid and sensitive method for the quantitation of microgram quantities of protein utilizing the principle of protein–dye binding. Anal. Biochem. 72, 248–254. http://dx.doi.org/10.1016/0003-2697(76)90527-3.

Brauner, C.J., Wang, T., Wang, Y., Richards, J.G., Gonzalez, R.J., Bernier, N.J., Xi, W., Patrick, M., Val, A.L., 2004. Limited extracellular but complete intracellular acid–base regulation during short-term environmental hypercapnia in the armoured catfish, *Liposarcus pardalis*. J. Exp. Biol. 207, 3381–3390. http://dx.doi.org/10.1242/jeb.01144.

Caldeira, K., Wickett, M.E., 2005. Ocean model predictions of chemistry changes from carbon dioxide emissions to the atmosphere and ocean. J. Geophys. Res. 110, C09S04. http://dx.doi.org/10.1029/2004JC002671.

Catches, J.S., Burns, J.M., Edwards, S.L., Claiborne, J.B., 2006. Na^+/H^+ antiporter, V-H^+-ATPase and Na^+/K^+-ATPase immunolocalization in a marine teleost (*Myoxocephalus octodecemspinosus*). J. Exp. Biol. 209, 3440–3447. http://dx.doi.org/10.1242/jeb.02384.

Claiborne, J.B., Blackston, C.R., Choe, K.P., Dawson, D.C., Harris, S.P., Mackenzie, L.A., Morrison-Shetlar, A.I., 1999. A mechanism for branchial acid excretion in marine fish: identification of multiple Na^+/H^+ antiporter (NHE) isoforms in gills of two seawater teleosts. J. Exp. Biol. 202, 315–324.

Claiborne, J.B., Edwards, S.L., Morrison-Shetlar, A.I., 2002. Acid–base regulation in fishes: cellular and molecular mechanisms. J. Exp. Zool. 293, 302–319. http://dx.doi.org/10.1002/jez.10125.

Collins, M., Knutti, R., Arblaster, J., Dufresne, J.-L., Fichefet, T., Friedlingstein, P., Gao, X., Gutowski, W.J., Johns, T., Krinner, G., Shongwe, M., Tebaldi, C., Weaver, A.J., Wehner, M., 2013. Long-term climate change: projections, commitments and irreversibility. In: Stocker, T.F., Qin, D., Plattner, G.K., Tignor, M., Allen, S.K., Boschung, J., Nauels, A., Xia, Y., Bex, V., Midgley, P.M. (Eds.), Climate Change 2013: The Physical Science BasisContribution of Working Group I to the Fifth Assessment Report of the Intergovernmental Panel on Climate Change.Cambridge University Press, Cambridge; United Kingdom and New York, NY, USA.

Conesa, A., Götz, S., García-Gómez, J.M., Terol, J., Talón, M., Robles, M., 2005. Blast2GO: a universal tool for annotation, visualization and analysis in functional genomics research. Bioinformatics 21, 3674–3676. http://dx.doi.org/10.1093/bioinformatics/bti610.

Cutler, C.P., Cramb, G., 2002. Two isoforms of the $Na^+/K^+/2Cl^-$ cotransporter are expressed in the European eel (*Anguilla anguilla*). Biochim. Biophys. Acta 1566, 92–103. http://dx.doi.org/10.1016/S0005-2736(02)00596-5.

Deigweiher, K., Koschnick, N., Pörtner, H.-O., Lucassen, M., 2008. Acclimation of ion regulatory capacities in gills of marine fish under environmental hypercapnia. Am. J. Physiol. Regul. Integr. Comp. Physiol. 295, R1660–R1670. http://dx.doi.org/10.1152/ajpregu.90403.2008.

Dorey, N., Lançon, P., Thorndyke, M., Dupont, S., 2013. Assessing physiological tipping point of sea urchin larvae exposed to a broad range of pH. Glob. Chang. Biol. 19, 3355–3367. http://dx.doi.org/10.1111/gcb.12276.

Epskamp, S., Cramer, A.O.J., Waldorp, L.J., Schmittmann, V.D., Borsboom, D., 2012. qgraph: network visualizations of relationships in psychometric data. J. Stat. Softw. 48, 1–18. http://dx.doi.org/10.18637/jss.v048.i04.

Esbaugh, A.J., Heuer, R., Grosell, M., 2012. Impacts of ocean acidification on respiratory gas exchange and acid–base balance in a marine teleost, *Opsanus beta*. J. Comp. Physiol. B. 182, 921–934. http://dx.doi.org/10.1007/s00360-012-0668-5.

Evans, D.H., Piermarini, P.M., Choe, K.P., 2005. The multifunctional fish gill: dominant site of gas exchange, osmoregulation, acid–base regulation, and excretion of nitrogenous waste. Physiol. Rev. 85, 97–177. http://dx.doi.org/10.1152/physrev.00050.2003.

Flicek, P., Amode, M.R., Barrell, D., Beal, K., Billis, K., Brent, S., Carvalho-Silva, D., Clapham, P., Coates, G., Fitzgerald, S., Gil, L., Girón, C.G., Gordon, L., Hourlier, T., Hunt, S., Johnson, N., Juettemann, T., Kähäri, A.K., Keenan, S., Kulesha, E., Martin, F.J., Maurel, T., McLaren, W.M., Murphy, D.N., Nag, R., Overduin, B., Pignatelli, M., Pritchard, B., Pritchard, E., Riat, H.S., Ruffier, M., Sheppard, D., Taylor, K., Thormann, A., Trevanion, S.J., Vullo, A., Wilder, S.P., Wilson, M., Zadissa, A., Aken, B.L., Birney, E., Cunningham, F., Harrow, J., Herrero, J., Hubbard, T.J.P., Kinsella, R., Muffato, M., Parker, A., Spudich, G., Yates, A., Zerbino, D.R., Searle, S.M.J., 2014. Ensembl 2014. Nucleic Acids Res. 42, D749–D755. http://dx.doi.org/10.1093/nar/gkt1196.

Hayashi, M., Kikkawa, T., Ishimatsu, A., 2013. Morphological changes in branchial mitochondria-rich cells of the teleost *Paralichthys olivaceus* as a potential indicator of CO_2 impacts. Mar. Pollut. Bull. 73, 409–415. http://dx.doi.org/10.1016/j.marpolbul.2013.06.034.

Heuer, R., Grosell, M., 2014. Physiological impacts of elevated carbon dioxide and ocean acidification on fish. Am. J. Physiol. Regul. Integr. Comp. Physiol. 307, R1061–R1084. http://dx.doi.org/10.1152/ajpregu.00064.2014.

Hirata, T., Kaneko, T., Ono, T., Nakazato, T., Furukawa, N., Hasegawa, S., Wakabayashi, S., Shigekawa, M., Chang, M.-H., Romero, M.F., Hirose, S., 2003. Mechanism of acid adaptation of a fish living in a pH 3.5 lake. Am. J. Physiol. Regul. Integr. Comp. Physiol. 284, R1199–R1212. http://dx.doi.org/10.1152/ajpregu.00267.2002.

Hiroi, J., McCormick, S.D., 2007. Variation in salinity tolerance, gill Na^+/K^+-ATPase, $Na^+/K^+/2Cl^-$ cotransporter and mitochondria-rich cell distribution in three salmonids *Salvelinus namaycush*, *Salvelinus fontinalis* and *Salmo salar*. J. Exp. Biol. 210, 1015–1024. http://dx.doi.org/10.1242/jeb.002030.

Hiroi, J., McCormick, S.D., 2012. New insights into gill ionocyte and ion transporter function in euryhaline and diadromous fish. Respir. Physiol. Neurobiol. 184, 257–268. http://dx.doi.org/10.1016/j.resp.2012.07.019.

Hu, M.Y., Guh, Y.-J., Stumpp, M., Lee, J.-R., Chen, R.-D., Sung, P.-H., Chen, Y.-C., Hwang, P.-P., Tseng, Y.-C., 2014. Branchial NH_4^+-dependent acid–base transport mechanisms and energy metabolism of squid (*Sepioteuthis lessoniana*) affected by seawater acidification. Front. Zool. 11, 55. http://dx.doi.org/10.1186/s12983-014-0055-z.

Hwang, P.-P., Lee, T.-H., Lin, L.-Y., 2011. Ion regulation in fish gills: recent progress in the cellular and molecular mechanisms. Am. J. Physiol. Regul. Integr. Comp. Physiol. 301, R28–R47. http://dx.doi.org/10.1152/ajpregu.00047.2011.

IPCC, 2013. Summary for policymakers. In: Stocker, T.F., Qin, D., Plattner, G.-K., Tignor, M., Allen, S.K., Boschung, J., Nauels, A., Xia, Y., Bex, V., Midgley, P.M. (Eds.), Climate Change 2013: The Physical Science BasisContribution of Working Group I to the Fifth Assessment Report of the Intergovernmental Panel on Climate Change. Cambridge University Press, Cambridge, United Kingdom and New York, NY, USA.

Kang, C.-K., Liu, F.-C., Chang, W.-B., Lee, T.-H., 2011. Effects of low environmental salinity on the cellular profiles and expression of Na^+, K^+-ATPase and Na^+, K^+, $2Cl^-$ cotransporter 1 of branchial mitochondrion-rich cells in the juvenile marine fish *Monodactylus argenteus*. Fish Physiol. Biochem. 38, 665–678. http://dx.doi.org/10.1007/s10695-011-9549-1.

Kreiss, C.M., Michael, K., Bock, C., Lucassen, M., Pörtner, H.-O., 2015a. Impact of long-term moderate hypercapnia and elevated temperature on the energy budget of isolated gills of Atlantic cod (*Gadus morhua*). Comp. Biochem. Physiol. A Mol. Integr. Physiol. 182, 102–112. http://dx.doi.org/10.1016/j.cbpa.2014.12.019.

Kreiss, C.M., Michael, K., Lucassen, M., Jutfelt, F., Motyka, R., Dupont, S., Pörtner, H.-O., 2015b. Ocean warming and acidification modulate energy budget and gill ion regulatory mechanisms in Atlantic cod (*Gadus morhua*). J. Comp. Physiol. B. 185, 767–781. http://dx.doi.org/10.1007/s00360-015-0923-7.

Laemmli, U.K., 1970. Cleavage of structural proteins during the assembly of the head of bacteriophage T4. Nature 227, 680–685. http://dx.doi.org/10.1038/227680a0.

Larsen, B.K., Pörtner, H.-O., Jensen, F.B., 1997. Extra- and intracellular acid–base balance and ionic regulation in cod (*Gadus morhua*) during combined and isolated exposures to hypercapnia and copper. Mar. Biol. 128, 337–346. http://dx.doi.org/10.1007/s002270050099.

Lee, T.-H., Tsai, J.C., Fang, M.J., Yu, M.J., Hwang, P.-P., 1998. Isoform expression of Na^+-K^+-ATPase α-subunit in gills of the teleost *Oreochromis mossambicus*. Am. J. Physiol. Regul. Integr. Comp. Physiol. 275, R926–R932.

Lorin-Nebel, C., Avarre, J.-C., Faivre, N., Wallon, S., Charmantier, G., Durand, J.-D., 2012. Osmoregulatory strategies in natural populations of the black-chinned tilapia *Sarotherodon melanotheron* exposed to extreme salinities in West African estuaries. J. Comp. Physiol. B. 182, 771–780. http://dx.doi.org/10.1007/s00360-012-0657-8.

Lucassen, M., Koschnick, N., Eckerle, L.G., Pörtner, H.O., 2006. Mitochondrial mechanisms of cold adaptation in cod (*Gadus morhua* L.) populations from different climatic zones. J. Exp. Biol. 209, 2462–2471. http://dx.doi.org/10.1242/jeb.02268.

Madsen, S.S., Kiilerich, P., Tipsmark, C.K., 2008. Multiplicity of expression of Na+, K + -ATPase α-subunit isoforms in the gill of Atlantic salmon (*Salmo salar*): cellular localisation and absolute quantification in response to salinity change. J. Exp. Biol. 212, 78–88. http://dx.doi.org/10.1242/jeb.024612.

Mark, F.C., Lucassen, M., Pörtner, H.-O., 2006. Thermal sensitivity of uncoupling protein expression in polar and temperate fish. Comp. Biochem. Physiol. D Genomics Proteomics 1, 365–374. http://dx.doi.org/10.1016/j.cbd.2006.08.004.

Marshall, W.S., Grosell, M., 2006. Ion transport, osmoregulation, and acid–base balance. In: Claiborne, J.B., Evans, D.H. (Eds.), The Physiology of Fishes. CRC Press, Boca Raton, FL, USA.

Meinshausen, M., Smith, S.J., Calvin, K., Daniel, J.S., Kainuma, M.L.T., Lamarque, J.-F., Matsumoto, K., Montzka, S.A., Raper, S.C.B., Riahi, K., Thomson, A., Velders, G.J.M., van Vuuren, D.P.P., 2011. The RCP greenhouse gas concentrations and their extensions from 1765 to 2300. Clim. Chang. 109, 213–241. http://dx.doi.org/10.1007/s10584-011-0156-z.

Melzner, F., Göbel, S., Langenbuch, M., Gutowska, M.A., Pörtner, H.-O., Lucassen, M., 2009a. Swimming performance in Atlantic cod (*Gadus morhua*) following long-term (4–12 months) acclimation to elevated seawater P_{CO2}. Aquat. Toxicol. 92, 30–37. http://dx.doi.org/10.1016/j.aquatox.2008.12.011.

Melzner, F., Gutowska, M.A., Langenbuch, M., Dupont, S., Lucassen, M., Thorndyke, M.C., Bleich, M., Pörtner, H.-O., 2009b. Physiological basis for high CO_2 tolerance in marine ectothermic animals: pre-adaptation through lifestyle and ontogeny? Biogeosciences 6, 2313–2331. http://dx.doi.org/10.5194/bg-6-2313-2009.

Michaelidis, B., Spring, A., Pörtner, H.-O., 2007. Effects of long-term acclimation to environmental hypercapnia on extracellular acid–base status and metabolic capacity in Mediterranean fish *Sparus aurata*. Mar. Biol. 150, 1417–1429. http://dx.doi.org/10.1007/s00227-006-0436-8.

Olsvik, P.A., Søfteland, L., Lie, K.K., 2008. Selection of reference genes for qRT-PCR examination of wild populations of Atlantic cod *Gadus morhua*. BMC Res. Notes 1, 47. http://dx.doi.org/10.1186/1756-0500-1-47.

Pelis, R.M., Zydlewski, J., McCormick, S.D., 2001. Gill Na^+-K^+-$2Cl^-$ cotransporter abundance and location in Atlantic salmon: effects of seawater and smolting. Am. J. Physiol. Regul. Integr. Comp. Physiol. 280, R1844–R1852.

Perry, S.F., Gilmour, K.M., 2006. Acid–base balance and CO_2 excretion in fish: unanswered questions and emerging models. Respir. Physiol. Neurobiol. 154, 199–215. http://dx.doi.org/10.1016/j.resp.2006.04.010.

Perry, S.F., Furimsky, M., Bayaa, M., Georgalis, T., Shahsavarani, A., Nickerson, J.G., Moon, T.W., 2003. Integrated responses of Na^+/HCO_3^- cotransporters and V-type H^+-ATPases in the fish gill and kidney during respiratory acidosis. Biochim. Biophys. Acta 1618, 175–184. http://dx.doi.org/10.1016/j.bbamem.2003.09.015.

Perry, S.F., Vulesevic, B., Grosell, M., Bayaa, M., 2009. Evidence that SLC26 anion transporters mediate branchial chloride uptake in adult zebrafish (*Danio rerio*). Am. J. Physiol. Regul. Integr. Comp. Physiol. 297, R988–R997. http://dx.doi.org/10.1152/ajpregu.00327.2009.

Perry, S.F., Braun, M.H., Genz, J., Vulesevic, B., Taylor, J.R., Grosell, M., Gilmour, K.M., 2010. Acid–base regulation in the plainfin midshipman (*Porichthys notatus*): an aglomerular marine teleost. J. Comp. Physiol. B. 180, 1213–1225. http://dx.doi.org/10.1007/s00360-010-0492-8.

Piermarini, P.M., Verlander, J.W., Royaux, I.E., Evans, D.H., 2002. Pendrin immunoreactivity in the gill epithelium of a euryhaline elasmobranch. Am. J. Physiol. Regul. Integr. Comp. Physiol. 283, R983–R992. http://dx.doi.org/10.1152/ajpregu.00178.2002.

Pörtner, H.-O., 2008. Ecosystem effects of ocean acidification in times of ocean warming: a physiologist's view. Mar. Ecol. Prog. Ser. 373, 203–217. http://dx.doi.org/10.3354/meps07768.

Pörtner, H.-O., 2012. Integrating climate-related stressor effects on marine organisms: unifying principles linking molecule to ecosystem-level changes. Mar. Ecol. Prog. Ser. 470, 273–290. http://dx.doi.org/10.3354/meps10123.

Pörtner, H.-O., Berdal, B., Blust, R., Brix, O., Colosimo, A., De Wachter, B., Giuliani, A., Johansen, T., Fischer, T., Knust, R., Lannig, G., Naevdal, G., Nedenes, A., Nyhammer, G., Sartoris, F.J., Serendero, I., Sirabella, P., Thorkildsen, S., Zakhartsev, M.V., 2001. Climate induced temperature effects on growth performance, fecundity and recruitment in marine fish: developing a hypothesis for cause and effect relationships in Atlantic cod (*Gadus morhua*) and common eelpout (*Zoarces viviparus*). Cont. Shelf Res. 21, 1975–1997. http://dx.doi.org/10.1016/S0278-4343(01)00038-3.

Powell, S., Szklarczyk, D., Trachana, K., Roth, A., Kuhn, M., Muller, J., Arnold, R., Rattei, T., Letunic, I., Doerks, T., Jensen, L.J., von Mering, C., Bork, P., 2012. eggNOG v3.0: orthologous groups covering 1133 organisms at 41 different taxonomic ranges. Nucleic Acids Res. 40, D284–D289. http://dx.doi.org/10.1093/nar/gkr1060.

Pritchard, J.B., 2003. The gill and homeostasis: transport under stress. Am. J. Physiol. Regul. Integr. Comp. Physiol. 285, R1269–R1271. http://dx.doi.org/10.1152/ajpregu.00516.2003.

R Core Team, 2014. R: A language and environment for statistical computing. R Foundation for Statistical Computing, Vienna, Austria URL http://www.R-project.org/.

Richards, J.G., Semple, J.W., Bystriansky, J.S., Schulte, P.M., 2003. Na^+/K^+-ATPase α-isoform switching in gills of rainbow trout (*Oncorhynchus mykiss*) during salinity transfer. J. Exp. Biol. 206, 4475–4486. http://dx.doi.org/10.1242/jeb.00701.

Righton, D.A., Andersen, K.H., Neat, F., Thorsteinsson, V., Steingrund, P., Svedäng, H., Michalsen, K., Hinrichsen, H.-H., Bendall, V., Neuenfeldt, S., Wright, P., Jonsson, P., Huse, G., van der Kooij, J., Mosegaard, H., Hüssy, K., Metcalfe, J., 2010. Thermal niche of Atlantic cod *Gadus morhua*: limits, tolerance and optima. Mar. Ecol. Prog. Ser. 420, 1–13. http://dx.doi.org/10.3354/meps08889.

Rimoldi, S., Terova, G., Brambilla, F., Bernardini, G., Gornati, R., Saroglia, M., 2009. Molecular characterization and expression analysis of Na^+/H^+ exchanger (NHE)-1 and c-Fos genes in sea bass (*Dicentrarchus labrax*, L) exposed to acute and chronic hypercapnia. J. Exp. Mar. Biol. Ecol. 375, 32–40. http://dx.doi.org/10.1016/j.jembe.2009.05.002.

Riou, V., Ndiaye, A., Budzinski, H., Dugué, R., Le Ménach, K., Combes, Y., Bossus, M., Durand, J.-D., Charmantier, G., Lorin-Nebel, C., 2012. Impact of environmental DDT concentrations on gill adaptation to increased salinity in the tilapia *Sarotherodon melanotheron*. Comp. Biochem. Physiol. C Toxicol. Pharmacol. 156, 7–16. http://dx.doi.org/10.1016/j.cbpc.2012.03.002.

Star, B., Nederbragt, A.J., Jentoft, S., Grimholt, U., Malmstrøm, M., Gregers, T.F., Rounge, T.B., Paulsen, J., Solbakken, M.H., Sharma, A., Wetten, O.F., Lanzén, A., Winer, R., Knight, J., Vogel, J.-H., Aken, B., Andersen, O., Lagesen, K., Tooming-Klunderud, A., Edvardsen, R.B., Tina, K.G., Espelund, M., Nepal, C., Previti, C., Karlsen, B.O., Moum, T., Skage, M., Berg, P.R., Gjøen, T., Kuhl, H., Thorsen, J., Malde, K., Reinhardt, R., Du, L., Johansen, S.D., Searle, S., Lien, S., Nilsen, F., Jonassen, I., Omholt, S.W., Stenseth, N.C., Jakobsen, K.S., 2011. The genome sequence of Atlantic cod reveals a unique immune system. Nature 477, 207–210. http://dx.doi.org/10.1038/nature10342.

Tipsmark, C.K., Madsen, S.S., Seidelin, M., Christensen, A.S., Cutler, C.P., Cramb, G., 2002. Dynamics of Na^+, K^+, $2Cl^-$ cotransporter and Na^+, K^+-ATPase expression in the branchial epithelium of brown trout (*Salmo trutta*) and Atlantic salmon (*Salmo salar*). J. Exp. Zool. 293, 106–118. http://dx.doi.org/10.1002/jez.10118.

Tipsmark, C.K., Luckenbach, J.A., Madsen, S.S., Kiilerich, P., Borski, R.J., 2008. Osmoregulation and expression of ion transport proteins and putative claudins in the gill of Southern Flounder (*Paralichthys lethostigma*). Comp. Biochem. Physiol. A Mol. Integr. Physiol. 150, 265–273. http://dx.doi.org/10.1016/j.cbpa.2008.03.006.

Tipsmark, C.K., Breves, J.P., Seale, A.P., Lerner, D.T., Hirano, T., Grau, E.G., 2011. Switching of Na^+, K^+-ATPase isoforms by salinity and prolactin in the gill of a cichlid fish. J. Endocrinol. 209, 237–244. http://dx.doi.org/10.1530/JOE-10-0495.

Toews, D.P., Holeton, G.F., Heisler, N., 1983. Regulation of the acid–base status during environmental hypercapnia in the marine teleost fish *Conger conger*. J. Exp. Biol. 107, 9–20.

Tse, C.-M., Levine, S.A., Yun, C.H.C., Khurana, S., Donowitz, M., 1994. Na^+/H^+ exchanger-2 is an 0-linked but not an O-linked sialoglycoprotein. Biochemistry 33, 12954–12961.

Tseng, Y.-C., Hu, M.Y., Stumpp, M., Lin, L.-Y., Melzner, F., Hwang, P.-P., 2013. CO_2-driven seawater acidification differentially affects development and molecular plasticity along life history of fish (*Oryzias latipes*). Comp. Biochem. Physiol. A Mol. Integr. Physiol. 165, 119–130. http://dx.doi.org/10.1016/j.cbpa.2013.02.005.

Watson, C.J., Nordi, W.M., Esbaugh, A.J., 2014. Osmoregulation and branchial plasticity after acute freshwater transfer in red drum, *Sciaenops ocellatus*. Comp. Biochem. Physiol. A Mol. Integr. Physiol. 178, 82–89. http://dx.doi.org/10.1016/j.cbpa.2014.08.008.

Weiss, M., Heilmayer, O., Brey, T., Lucassen, M., Pörtner, H.-O., 2012. Physiological capacity of *Cancer setosus* larvae—adaptation to El Niño southern oscillation conditions. J. Exp. Mar. Biol. Ecol. 413, 100–105. http://dx.doi.org/10.1016/j.jembe.2011.11.023.

Windisch, H.S., Lucassen, M., Frickenhaus, S., 2012. Evolutionary force in confamiliar marine vertebrates of different temperature realms: adaptive trends in zoarcid fish transcriptomes. BMC Genomics 13, 549. http://dx.doi.org/10.1186/1471-2164-13-549.